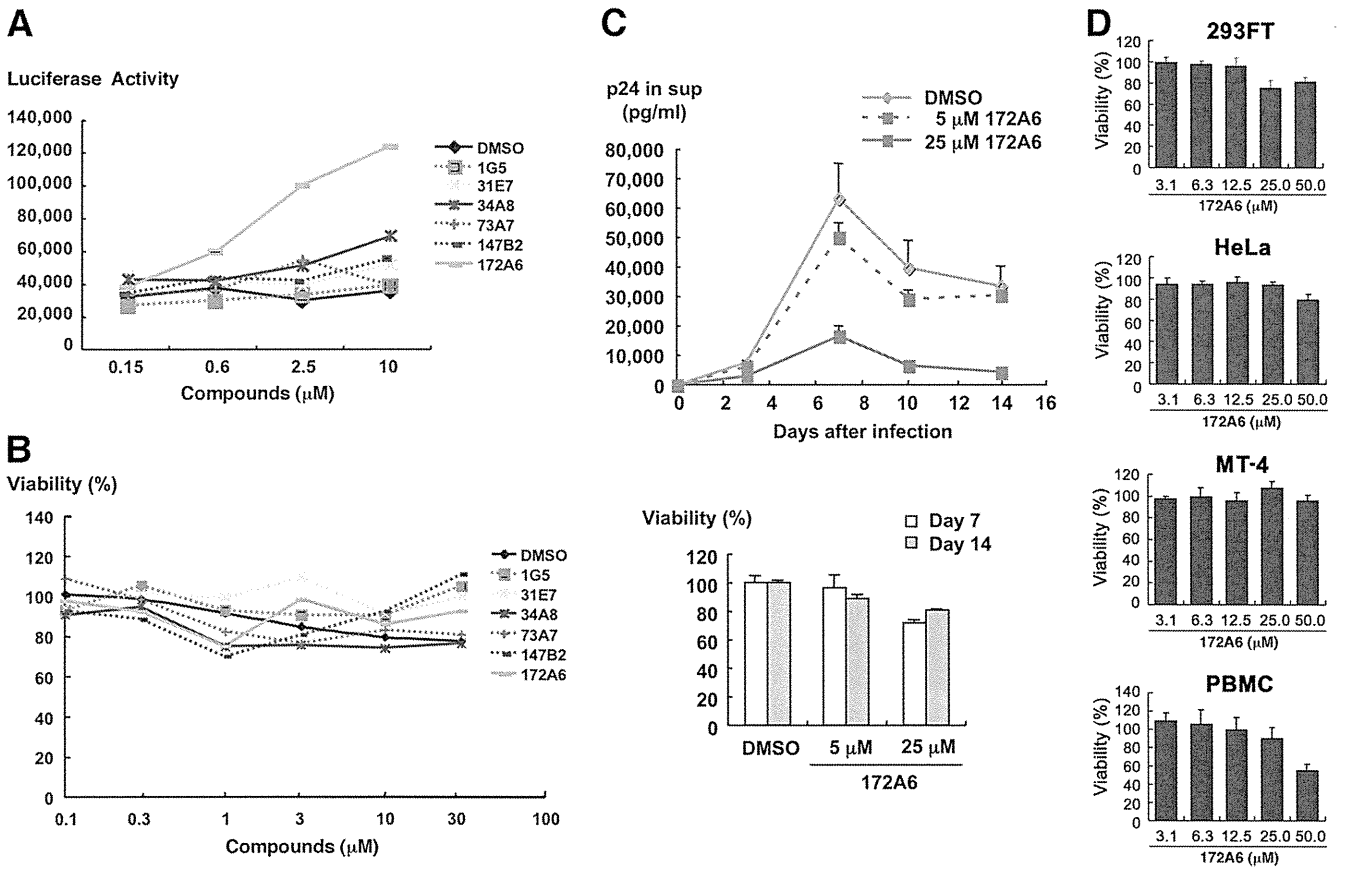

FIG. 3. Inhibition of HIV-1 replication and cell toxicity. (A) MT-4 Luc cells were infected with HIV-1 (HXB2 strain) and incubated at 37°C in the presence of increasing doses of compounds. On day 7, MT-4 Luc cells were subjected to luciferase assay. Data were shown as means from triplicate cultures. (B) 293T cells were incubated with various doses of compounds at 37°C for 2 days and subjected to Alamar Blue assays. Data were shown as means from 3 independent experiments. (C) PBMC stimulated with IL-2 and anti-CD3 antibody were infected with HIV-1 (HXB2 strain) and incubated at 37°C in the presence of 5 and 25 μM 172A6. HIV-1 production in culture medium was temporally quantified by p24CA antigen capture ELISA (top). Uninfected PBMC were cultured with 172A6 at 37°C and were subjected to MTS assay on days 7 and 14. Data were shown as means with standard deviations from triplicate cultures, in which DMSO was used as control. (D) 293FT, HeLa, and MT-4 cells and PBMC were incubated at 37°C with various doses of 172A6 and were subjected to MTS assay on days 4, 3, 4, and 6, respectively. Cell viability was shown as OD_{490}. Data were shown as means with standard deviations from triplicate cultures.

microscopy (Fig. 4B). HeLa cells were transfected with a pNL43 derivative that expresses Gag-GFP and incubated with 30 μM BMMP. Gag-GFP was distributed predominantly at the plasma membrane in cells treated with DMSO (used as control). A similar Gag-GFP distribution was observed in cells treated with BMMP, indicating that BMMP did not inhibit Gag targeting to the plasma membrane, consistent with the above findings.

Inhibition of HIV replication postentry by BMMP. To examine whether BMMP exerted an inhibitory effect on early stages of the HIV life cycle, such as viral entry, we employed single-round infection assays with luciferase-expressing HIV-1 vectors which were pseudotyped with either VSV-G or authentic HIV-1 Env protein. To this end, pHIVgag-pol (for expression of HIV-1 Gag and Gag-Pol), pRevpac (for expression of HIV-1 Rev), and pLenti-luciferase vector, which provides the artificial lentiviral genome expressing luciferase driven by cytomegalovirus promoter, were cotransfected with either VSV-G or authentic HIV-1 Env expression plasmid into 293FT cells. HIV-1 Luc viruses produced were inoculated into MT-4 cells in the presence of BMMP, and viral infectivity was monitored by a luciferase reporter assay. Luciferase expression was inhibited in a BMMP dose-dependent manner in cells infected with the HIV-1 Env-pseudotyped Luc virus, indicating that BMMP inhibited the early stage of the HIV-1 life cycle (Fig. 5A). However, when VSV-G-pseudotyped Luc virus was used, a dose-dependent reduction was similarly observed. When HIV-1 (NL43 strain) expressing luciferase was pseudotyped with VSV-G and used in this assay, the luciferase activity driven by the LTR promoter was similarly reduced in the presence of BMMP, suggesting that BMMP did not inhibit the stage of HIV entry (e.g., attachment and membrane fusion processes) but the stage of postentry (e.g., uncoating) (Fig. 5A). The Env-independent infectivity reduction was confirmed when HIV-1 Luc viruses were inoculated into 293FT and 293FT-CD4 cells (Fig. 5B). We examined whether BMMP also blocked the postentry stage of SIV. Interestingly, single-round infection assays with luciferase-expressing SIVmac239 vectors which were pseudotyped with VSV-G protein showed no inhibition of luciferase expres-

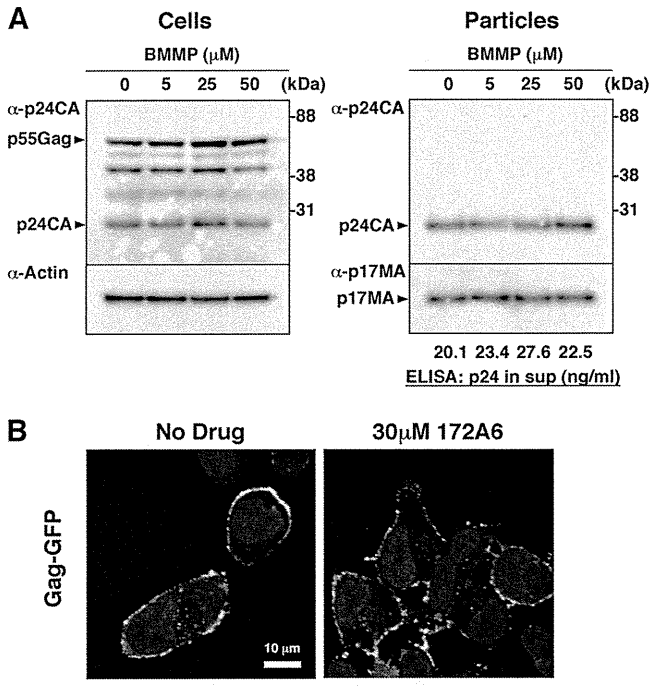

FIG. 4. HIV-1 particle production and Gag plasma membrane targeting. (A) Effects on HIV-1 particle production. 293FT cells were transfected with pHXB2 and incubated at 37°C with 0 to 50 μM BMMP. Two days posttransfection, cells were collected and culture media were subjected to purification of viral particles by ultracentrifugation. Equivalent volumes of samples were subjected to SDS-PAGE followed by Western blotting using anti-HIV-1 p24CA antibody. Representative blots were shown. HIV-1 particle yields in culture media were quantified by p24CA antigen capture ELISA. (B) Intracellular localization of Gag. HeLa cells were transfected with a pNL43 derivative in which Gag was fused with GFP and incubated at 37°C for 1.5 days with 30 μM BMMP. Nuclei were stained with TO-PRO-3, and cells were observed by confocal microscopy. Representative images were shown at the same magnification. Bar = 10 μm.

sion (Fig. 5B). No reduction in luciferase expression was also observed when luciferase-expressing pseudotyped MLV was used (data not shown). These data suggest that BMMP specifically inhibits HIV replication postentry but not those of other retroviruses, such as SIV and MLV.

To confirm the postentry block prior to particle production, we isolated cellular DNA from MT-4 cells infected with HIV-1 (HXB2 strain) that were treated with BMMP. Then, we quantified early reverse transcripts of HIV (corresponding to the strong-stop DNA), late reverse transcripts of HIV, and integrated HIV DNA by PCR. When normalized to the level of β-globin DNA (internal control), the levels of the early and late reverse transcripts and of the integrated proviral DNA were reduced, as observed for cells treated with 200 nM efavirenz controls (Fig. 5C). However, RT enzymatic activity was not affected by BMMP when examined in *in vitro* assays (data not shown). Together, these data indicate that BMMP blocks the early stage of the HIV-1 life cycle, preventing the completion of reverse transcription.

Mapping of Gag domain targeted by BMMP. To map the HIV Gag domain responsible for the postentry block by BMMP, a series of chimeric Gag constructs between HIV-1 and SIVmac239 were made in the context of pHIVgag-pol. HIV-1 MA, MACA, and CA were replaced by SIV MA, MACA, and CA, respectively (referred to as sMA, sMACA, and sCA, respectively). These Gag/Gag-Pol expression plasmids were cotransfected with pRevpac and pLenti-luciferase vector, and viruses were pseudotyped with VSV-G protein. Western blotting using anti-HIV-1 p17MA and p24CA and anti-SIVmac p27CA antibodies revealed that, although the anti-HIV-1 p24CA antibody that we used was cross-reactive with SIV CA, each domain of Gag was replaced in the chimeric constructs and virus particles were produced at levels largely similar to that of the wild type of HIV-1 Gag construct (Fig. 6A). Single-round infection assays with these Gag chimeras revealed that BMMP inhibited viral infection postentry only when HIV-1 CA was present in the constructs (Fig. 6B). Thus, our data indicated that BMMP inhibited the early stage of HIV-1 replication in a CA-specific and species-specific manner. These phenotypes resemble those observed for the CA-specific retroviral restriction imposed by a host factor, tripartite motif protein 5 (TRIM5) (30). HIV-1 CA is known to bind a host factor, CypA, likely through amino acids G89 and P90 in the exposed loop of CA (15, 16). This binding facilitates the early stage of HIV-1 replication prior to reverse transcription (9). Interestingly, HIV/SIV chimera studies have shown that the CypA-binding site overlaps with the determinants for species-specific restriction (30, 34). Thus, we made an HIV-1 Gag construct containing amino acid substitutions G89A and P90A in the CypA-binding loop of CA (referred to as CypA mt) and tested the sensitivity to BMMP. The CypA mt did not display the resistance to BMMP (Fig. 6B), suggesting that HIV-1 inhibition by BMMP was not linked to the CypA binding or TRIM5. No firm conclusions were drawn from mapping experiments using Gag chimeras within CA, i.e., N- and C-terminal domains (NTD and CTD), since the CTD mutant showed a lower yield of particle production (data not shown).

Disassembly of HIV capsid core by BMMP. The chimera experiments showed that the CA domain is critical for the inhibitory effect of BMMP on the early stage of HIV-1 replication. Thus, we examined whether BMMP affects CA-CA interaction using purified CA. An *in vitro* assembly reaction with purified HIV-1 CA was employed to test if BMMP disrupted CA-CA interactions. *In vitro* assembly reaction of CA has shown it to produce tubular structures representing the mature CA capsid structure (17, 36). We added BMMP to the *in vitro* assembly reaction with 100 μM HIV-1 CA, and resultant CA assembly products were observed by electron microscopy (Fig. 7A). For quantitative analysis, the resultant CA assembly products were recovered by ultracentrifugation and subjected to SDS-PAGE. The levels of the CA assembly products were reduced when BMMP was added at a concentration higher than 30 μM, corresponding to approximately a 1:3 molar ratio to CA (Fig. 7A). These data suggest that BMMP targets HIV-1 CA and leads to the destabilization of the viral capsid core, since our previous findings indicated that BMMP did not block particle release (Fig. 4) but did block the HIV-1 infection postentry (Fig. 5).

To test this possibility in a more relevant assay, we adopted cell-free disassembly assays using purified HIV-1 mature capsid core. To this end, we isolated HIV-1 capsid cores by ultracentrifugation through a Triton X-100 layer, as described pre-

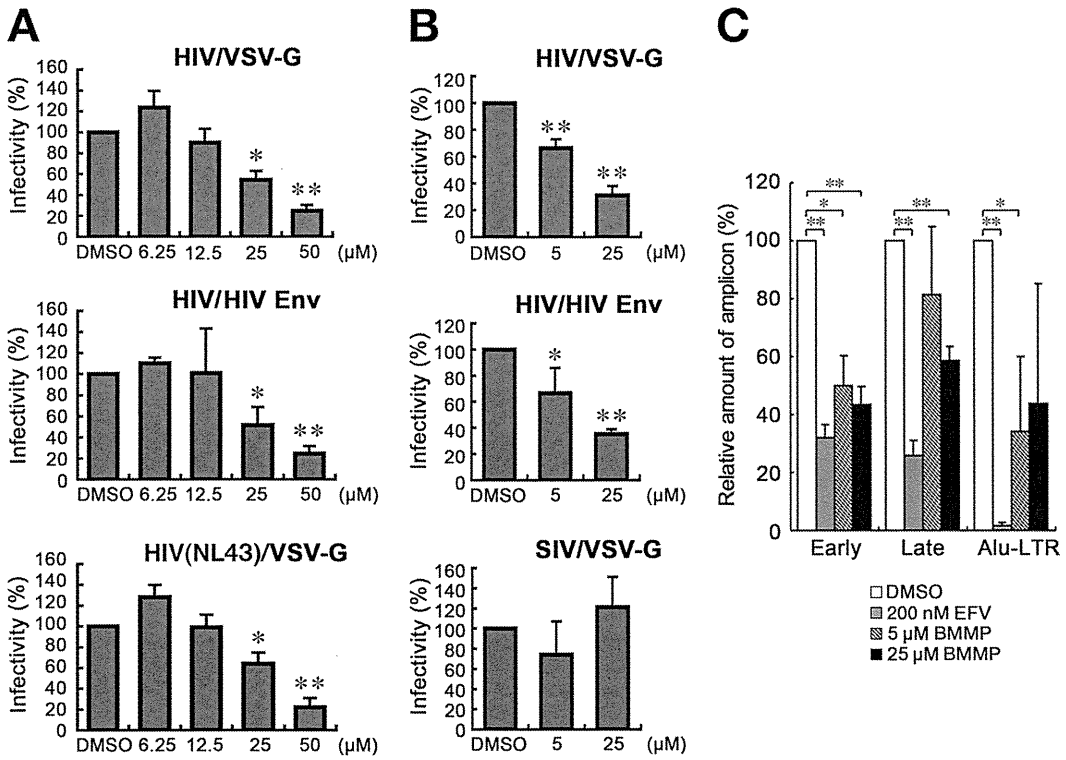

FIG. 5. Inhibition of HIV-1 replication postentry. (A) Single-round infection assays in MT-4 cells. 293FT cells were cotransfected with pHIVgag-pol (derived from HXB2 strain), pLenti-luciferase, pRevpac, and either a plasmid expressing HIV-1 Env (middle) or a plasmid expressing VSV-G (top). HIV-1 (NL43 strain) expressing luciferase was similarly pseudotyped with VSV-G protein (bottom). Following incubation, the culture supernatants were recovered and were subsequently inoculated into MT-4 cells with increasing doses of BMMP. (B) Single-round infection assays in 293FT and 293FT-CD4 cells. HIV-1 vectors containing the luciferase gene were similarly pseudotyped with HIV-1 Env (middle) or VSV-G protein (top). Luciferase-expressing SIVmac was pseudotyped with VSV-G protein by cotransfection (bottom). Viruses produced were subsequently inoculated into 293FT (top and bottom) or 293FT-CD4 (middle) cells with 5 and 25 μM BMMP. Viral infectivity was assessed by luciferase reporter assays. Data were shown as means with standard deviations from 3 to 6 independent experiments in panels A and B. *, $P < 0.05$; **, $P < 0.01$. (C) Quantitative PCR. MT-4 cells were infected with HIV-1 (HXB2 strain) and incubated in the presence of BMMP. DNA was isolated at 4 or 24 h postinfection and subjected to quantitative PCR for HIV cDNA. Reverse transcripts generated at the early and late phases of HIV reverse transcription were amplified from the DNA isolated at 4 and 24 h postinfection, respectively. The integrated viral genome was amplified as *Alu*-LTR transcripts from the DNA isolated at 24 h postinfection. EFV (200 nM) was used as positive controls. Three independent infections were performed, and quantitative PCR was carried out in triplicate with each infection sample. Representative data were shown with the means and standard deviations. *, $P < 0.05$; **, $P < 0.01$.

viously (3). HIV-1 cores are known to disassemble when incubated at 37°C. We examined if BMMP accelerated the rate of core disassembly. The HIV-1 cores were incubated with BMMP at 37°C up to 120 min, and residual intact cores were recovered by centrifugation. When quantified by p24CA antigen capture ELISA, intact cores were found to be reduced in a time-dependent manner in the presence of DMSO (as control), consistent with previous reports (3). A similar level of reduction was observed in the presence of AZT. However, addition of BMMP accelerated a reduction in intact cores in a dose-dependent manner (Fig. 7B). Altogether, our data indicated that BMMP disrupted HIV-1 capsid cores through targeting CA.

DISCUSSION

In this study, we employed a yeast membrane-associated two-hybrid assay to monitor the HIV Gag-Gag interactions and established cell-based screening assays for drugs targeting Gag assembly. We screened a commercially available chemical library and found BMMP, which inhibits HIV-1 replication in PBMC culture. Our single-round infection analysis indicated that BMMP primarily targets HIV-1 CA and inhibits HIV infection postentry but not particle production (Fig. 4 to 6). *In vitro* CA assembly/disassembly assays showed that BMMP facilitated HIV-1 core disassembly (Fig. 7). Collectively, it is conceivable that BMMP may bind to mature capsid structure and facilitate disassembly of the capsid, leading to premature earlier uncoating and failure of postentry events (e.g., reverse transcription and integration). The mechanism of action may be akin to the block of HIV-1 entry by rTRIM5α (30).

Previous studies have reported inhibitors that target HIV-1 Gag assembly and/or Gag processing. 3-*O*-(3′,3′-Dimethylsuccinyl)betulinic acid, known as PA-457 or Bevirimat (molecular weight, 584), binds to the Gag CA-SP1 cleavage site and inhibits proteolytic conversion of Gag precursors to the mature form of p24CA (50% inhibitory concentration [IC_{50}] = 10 nM) (1, 2, 21). Inhibition of Gag processing has also been observed with a distinct chemical class of compound, 1-[2-(4-tert-butylphenyl)-2-(2,3-dihydro-1H-inden-2-ylamino)ethyl]-3-(trifluoro-

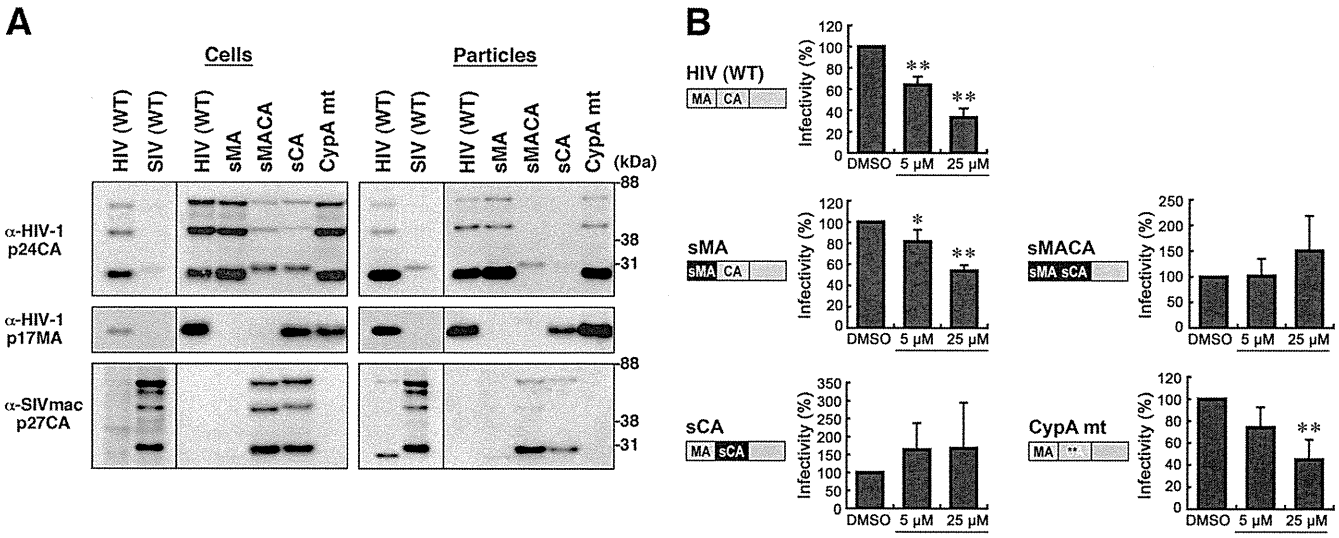

FIG. 6. Mapping of Gag domain responsible for inhibition. (A) Intracellular Gag expression and particle production. 293FT cells were cotransfected with pHIVgag-pol expressing chimeric Gag, pLenti-luciferase, pRevpac, and a plasmid expressing VSV-G, and virus particles produced were purified by ultracentrifugation. Cells and particles were analyzed by Western blotting using anti-HIV-1 p24CA and p17MA and anti-SIVmac p27CA antibodies. (B) Single-round infection assays with the Gag domain chimeras and Gag mutants with amino acid substitutions. The corresponding domain of SIVmac Gag (black) was introduced into HIV-1 Gag background (gray), and the resultant chimera was referred to as "s" plus the name of the corresponding domain of SIVmac. WT, wild type; sMA, HIV containing replacement of MA with SIV MA; sMACA, HIV containing replacement of MACA with SIV MACA; sCA, HIV containing replacement of CA with SIV CA. CypA mt represents HIV with amino acid substitutions G89A and P90A in the CypA-binding loop of CA NTD (denoted by asterisks). Following infection, the cell culture was incubated in the presence of 5 and 25 μM BMMP. Viral infectivity was monitored by luciferase reporter assays. Data were shown as means with standard deviations from 4 to 6 independent experiments. *, $P < 0.05$; **, $P < 0.01$.

methyl)pyridin-2(1H)-one (molecular weight, 454) (7). The hallmark of these inhibitors is incomplete Gag processing and accumulation of processing intermediates (e.g., CA-SP1) in virions, resulting in the loss of viral infectivity. These compounds do not inhibit Gag assembly. Since our BMMP did not show alteration in overall patterns of Gag processing (Fig. 4A), it is unlikely that BMMP shares the inhibition mechanisms with above inhibitors.

Inhibitors of HIV capsid assembly have been extensively screened by several approaches. *In silico* screening from public chemical libraries has identified *N*-(3-chloro-4-methylphenyl)-*N'*-{2-[({5-[(dimethylamino)-methyl]-2-furyl}-methyl)-sulfanyl] ethyl}-urea, termed CAP-1 (32), which binds to HIV-1 CA NTD (K_d [dissociation constant] = 800 μM), resulting in the inhibition of the correct interaction of hexameric units of CA NTD with dimeric units of CA CTD, essential for a high order of CA assembly (20). CAP-1 reduced the infectivity of progeny HIV but did not inhibit viral entry or particle production (32). Phage display biopanning has also been employed and has isolated a 12-mer peptide, termed CAI, which binds to HIV-1 CA CTD (50% inhibitory concentration [IC_{50}] = 3 to 4 μM) and inhibits CA capsid formation *in vitro* (K_d = 15 μM) (5, 29, 33). However, CAI did not inhibit HIV replication in cell culture because of the lack of cell permeability. In a subsequent study, CAI has been converted to a cell-penetrating peptide (termed NYAD-1) by stabilizing the α-helical structure of CAI with a hydrocarbon staple, leading to a marked improvement of K_d (<1 μM) (38). Surprisingly, the study revealed that, besides inhibiting the particle production, NYAD-1 disrupted the mature core formation and inhibited the early stage of HIV-1 in single-round infection assays, suggesting that NYAD-1 may affect the uncoating stage of the HIV life cycle through a mechanism similar to that of BMMP.

The difference between BMMP and CAI/NYAD-1 is that BMMP does not affect HIV-1 particle production or maturation steps. This is possibly because BMMP inhibits CA-CA interactions more efficiently than Gag-Gag interactions. Importantly, BMMP is not a peptide but a low-molecular-weight compound (molecular weight, 273.38), which is chemically and physically stable. It should be possible to chemically modify the BMMP structure to potentiate its biochemical and biological activities. The advantage of BMMP is that, due to its low molecular weight, the derivatives could retain cell membrane permeability unless large chemical groups are attached to the core structure.

A low-molecular-weight Gag inhibitor, PF74, previously screened from a chemical library by a high-throughput single-round infection assay (6), has been characterized by a more recent study, in which PF74 selectively inhibited HIV-1 (27). PF74 destabilized HIV-1 capsids and inhibited the postentry events, similarly to BMMP, but at low-micromolar concentrations. However, BMMP is distinct from PF74 in that the CypA-binding loop is not involved in the viral susceptibility to BMMP (Fig. 6B). Also, BMMP did not reduce the viral infectivity when the virion was exposed to BMMP (data not shown). Therefore, BMMP may have a potential to serve as a lead compound for the development of anti-HIV drugs bearing a novel mechanism of action.

Although BMMP showed anti-HIV activity, it still needs to be improved to lower the IC_{50}. We suggest that comprehensive studies on structural analogues of BMMP would be informative to understand the structure-function relationship of

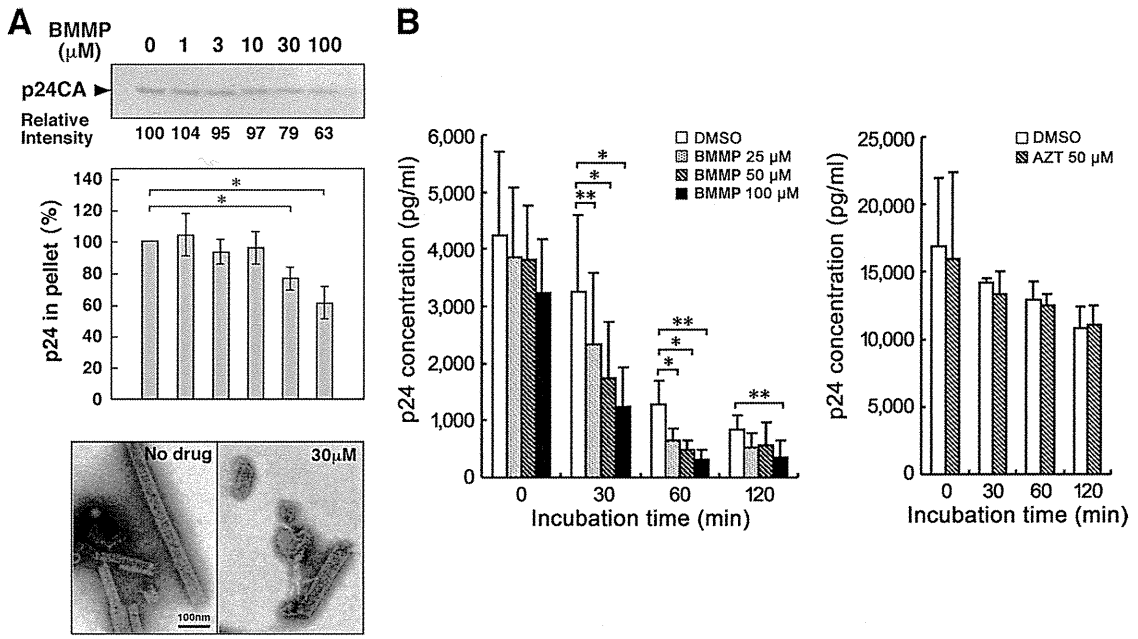

FIG. 7. HIV-1 mature capsid disassembly and *in vitro* assembly assays. (A) *In vitro* assembly reaction with purified HIV-1 CA. Purified HIV-1 CA protein (100 μM) was incubated with various doses of BMMP at 37°C for 60 min in buffer at high salt concentration. All samples included 1% DMSO. Assembly products were recovered by centrifugation and subjected to SDS-PAGE followed by Coomassie brilliant blue staining. The band intensities were semiquantified by ImageJ software. For quantification, the pelleted products were subjected to p24CA antigen capture ELISA. Data were shown as means with standard deviations from 3 independent experiments. *, $P < 0.05$. Assembly products were also negatively stained and examined by electron microscopy. Micrographs were shown at the same magnification. Bar = 100 nm. (B) Cell-free assays for HIV-1 uncoating. HIV-1 mature capsids were isolated through a 1% Triton X-100 layer as described previously (3). The HIV-1 cores were incubated with various doses of BMMP at 37°C up to 120 min. For comparison, the cores were similarly incubated with 50 μM AZT. All samples included 1% DMSO. Residual intact cores were recovered by ultracentrifugation and quantified by p24CA antigen capture ELISA. Data were shown as means with standard deviations from 4 independent experiments. *, $P < 0.05$; **, $P < 0.01$.

BMMP. Also, analysis of BMMP-resistant viruses and X-ray cocrystallography should provide insights into the mechanism of action that direct the way to potentiate the BMMP derivatives.

Recent cryo-electron microscopy and X-ray structure analysis have revealed the intermolecular interfaces between NTD and CTD in the three-dimensional hexameric structures of full-length CA (18, 24). It has been strongly suggested that multiple CA interactions, including NTD-NTD, CTD-CTD, and NTD-CTD, are essential for the constitution of mature HIV capsid. It is possible that some of the interfaces may not be formed in Gag-Gag interactions. CAI, similar to CAP-1, may inhibit CA assembly possibly by disrupting the formation of the NTD-CTD interface (18). Thus, these studies may provide a rationale for developing inhibitors that target the molecular interface of CA that specifically appears during a higher order of oligomerization. We suggest that viral capsid assembly/disassembly is an attractive therapeutic target and that such capsid inhibitors would help understand the regulation of postentry events.

ACKNOWLEDGMENTS

This work was supported by a Human Science grant from the Ministry of Health, Labor, and Welfare of Japan and by a Grant-in-Aid for Scientific Research from the Japan Society for the Promotion of Science.

REFERENCES

1. **Adamson, C. S., et al.** 2006. In vitro resistance to the human immunodeficiency virus type 1 maturation inhibitor PA-457 (Bevirimat). J. Virol. **80:** 10957–10971.
2. **Adamson, C. S., K. Waki, S. D. Ablan, K. Salzwedel, and E. O. Freed.** 2009. Impact of human immunodeficiency virus type 1 resistance to protease inhibitors on evolution of resistance to the maturation inhibitor bevirimat (PA-457). J. Virol. **83:**4884–4894.
3. **Aiken, C.** 2009. Cell-free assays for HIV-1 uncoating. Methods Mol. Biol. **485:**41–53.
4. **Aronheim, A., et al.** 1994. Membrane targeting of the nucleotide exchange factor Sos is sufficient for activating the Ras signaling pathway. Cell **78:**949–961.
5. **Bartonova, V., et al.** 2008. Residues in the HIV-1 capsid assembly inhibitor binding site are essential for maintaining the assembly-competent quaternary structure of the capsid protein. J. Biol. Chem. **283:**32024–32033.
6. **Blair, W. S., et al.** 2005. A novel HIV-1 antiviral high throughput screening approach for the discovery of HIV-1 inhibitors. Antiviral Res. **65:**107–116.
7. **Blair, W. S., et al.** 2009. New small-molecule inhibitor class targeting human immunodeficiency virus type 1 virion maturation. Antimicrob. Agents Chemother. **53:**5080–5087.
8. **Botstein, D.** 1997. Yeast as a model organism. Science **277:**1259–1260.
9. **Braaten, D., E. K. Franke, and J. Luban.** 1996. Cyclophilin A is required for an early step in the life cycle of human immunodeficiency virus type 1 before the initiation of reverse transcription. J. Virol. **70:**3551–3560.
10. **Broder, S.** 2010. The development of antiretroviral therapy and its impact on the HIV-1/AIDS pandemic. Antiviral Res. **85:**1–18.
11. **Bukovsky, A. A., A. Weimann, M. A. Accola, and H. G. Gottlinger.** 1997. Transfer of the HIV-1 cyclophilin-binding site to simian immunodeficiency virus from *Macaca mulatta* can confer both cyclosporin sensitivity and cyclosporin dependence. Proc. Natl. Acad. Sci. U. S. A. **94:**10943–10948.
12. **Butler, S. L., M. S. T. Hansen, and F. D. Bushman.** 2001. A quantitative assay for HIV DNA integration *in vivo*. Nat. Med. **7:**631–634.
13. **Craven, R. C., and L. J. Parent.** 1996. Dynamic interactions of the Gag polyprotein. Curr. Top. Microbiol. Immunol. **214:**65–94.
14. **Forshey, B. M., U. von Schwedler, W. I. Sundquist, and C. Aiken.** 2002.

Formation of a human immunodeficiency virus type 1 core of optimal stability is crucial for viral replication. J. Virol. **76:**5667–5677.
15. **Franke, E. K., H. E. Yuan, and J. Luban.** 1994. Specific incorporation of cyclophilin A into HIV-1 virions. Nature **372:**359–362.
16. **Gamble, T. R., et al.** 1996. Crystal structure of human cyclophilin A bound to the amino-terminal domain of HIV-1 capsid. Cell **87:**1285–1294.
17. **Ganser, B. K., S. Li, V. Y. Klishko, J. T. Finch, and W. I. Sundquist.** 1999. Assembly and analysis of conical models for the HIV-1 core. Science **283:** 80–83.
18. **Ganser-Pornillos, B. K., A. Cheng, and M. Yeager.** 2007. Structure of full-length HIV-1 CA: a model for the mature capsid lattice. Cell **131:**70–79.
19. **Graf Einsiedel, H., et al.** 2002. Deletion analysis of $p16^{INKa}$ and $p15^{INKb}$ in relapsed childhood acute lymphoblastic leukemia. Blood **99:**4629–4631.
20. **Kelly, B. N., et al.** 2007. Structure of the antiviral assembly inhibitor CAP-1 complex with the HIV-1 CA protein. J. Mol. Biol. **373:**355–366.
21. **Li, F., et al.** 2003. PA-457: a potent HIV inhibitor that disrupts core condensation by targeting a late step in Gag processing. Proc. Natl. Acad. Sci. U. S. A. **100:**13555–13560.
22. **Morikawa, Y.** 2003. HIV capsid assembly. Curr. HIV Res. **1:**1–14.
23. **Pauwels, R., et al.** 1990. Potent and selective inhibition of HIV-1 replication in vitro by a novel series of TIBO derivatives. Nature **343:**470–474.
24. **Pornillos, O., et al.** 2009. X-ray structures of the hexameric building block of the HIV capsid. Cell **137:**1282–1292.
25. **Roberts, N. A., et al.** 1990. Rational design of peptide-based HIV proteinase inhibitors. Science **248:**358–361.
26. **Sakuragi, S., T. Goto, K. Sano, and Y. Morikawa.** 2002. HIV type 1 Gag virus-like particle budding from spheroplasts of *Saccharomyces cerevisiae*. Proc. Natl. Acad. Sci. U. S. A. **99:**7956–7961.
27. **Shi, J., J. Zhou, V. B. Shah, C. Aiken, and K. Whitby.** 2011. Small molecule inhibition of human immunodeficiency virus type 1 infection by virus capsid destabilization. J. Virol. **85:**542–549.
28. **Shimizu, S., et al.** 2007. Inhibiting lentiviral replication by HEXIM1, a cellular negative regulator of the CDK9/cyclin T complex. AIDS **21:**575–582.
29. **Sticht, J., et al.** 2005. A peptide inhibitor of HIV-1 assembly *in vitro*. Nat. Struct. Mol. Biol. **12:**671–677.
30. **Stremlau, M., et al.** 2006. Specific recognition and accelerated uncoating of retroviral capsids by the TRIM5alpha restriction factor. Proc. Natl. Acad. Sci. U. S. A. **103:**5514–5519.
31. **Suzuki, S., et al.** 2010. Peptide HIV-1 integrase inhibitors from HIV-1 gene products. J. Med. Chem. **53:**5356–5360.
32. **Tang, C., et al.** 2003. Antiviral inhibition of the HIV-1 capsid protein. J. Mol. Biol. **327:**1013–1020.
33. **Ternois, F., J. Sticht, S. Duquerroy, H. G. Krausslich, and F. A. Rey.** 2005. The HIV-1 capsid protein C-terminal domain in complex with a virus assembly inhibitor. Nat. Struct. Mol. Biol. **12:**678–682.
34. **Towers, G. J., et al.** 2003. Cyclophilin A modulates the sensitivity of HIV-1 to host restriction factors. Nat. Med. **9:**1138–1143.
35. **Urano, E., et al.** 2008. Substitution of the myristoylation signal of human immunodeficiency virus type 1 Pr55Gag with the phospholipase C-delta1 pleckstrin homology domain results in infectious pseudovirion production. J. Gen. Virol. **89:**3144–3149.
36. **von Schwedler, U. K., et al.** 1998. Proteolytic refolding of the HIV-1 capsid protein amino-terminus facilitates viral core assembly. EMBO J. **17:**1555–1568.
37. **Westby, M., G. R. Nakayama, S. L. Butler, and W. S. Blair.** 2005. Cell-based and biochemical screening approaches for the discovery of novel HIV-1 inhibitors. Antiviral Res. **67:**121–140.
38. **Zhang, H., et al.** 2008. A cell-penetrating helical peptide as a potential HIV-1 inhibitor. J. Mol. Biol. **378:**565–580.

Gene Therapy (2011) 18, 936–941

www.nature.com/gt

SHORT COMMUNICATION

Protein transduction by pseudotyped lentivirus-like nanoparticles

T Aoki[1,2], K Miyauchi[1,2], E Urano[1], R Ichikawa[1] and J Komano[1]

A simple, efficient and reproducible method to transduce proteins into mammalian cells has not been established. Here we describe a novel protein transduction method based on a lentiviral vector. We have developed a method to package several thousand foreign protein molecules into a lentivirus-like nanoparticle (LENA) and deliver them into mammalian cells. In this proof-of-concept study, we used β-lactamase (BlaM) as a reporter molecule. The amino-terminus of BlaM was fused to the myristoylation signal of *lyn*, which was placed upstream of the amino-terminus of *Gag* (BlaM-gag-pol). By co-transfection of plasmids encoding BlaM-gag-pol and vesicular stomatitis virus-G (VSV-G) into 293T cells, LENA were produced containing BlaM enzyme molecules as many as Gag per capsid, which has been reported to be ~5000 molecules, but lacking the viral genome. Infection of 293T and MT-4 cells by VSV-G-pseudotyped BlaM-containing LENA led to successful transduction of BlaM molecules into the cell cytoplasm, as detected by cleavage of the fluorescent BlaM substrate CCF2-AM. LENA-mediated transient protein transduction does not damage cellular DNA, and the preparation of highly purified protein is not necessary. This technology is potentially useful in various basic and clinical applications.
Gene Therapy (2011) **18,** 936–941; doi:10.1038/gt.2011.38; published online 31 March 2011

Keywords: LENA; BlaM; Gag; protein transduction; lentiviral vector

INTRODUCTION

When viruses infect cells the viral contents are released. A virus can, therefore, be considered as a protein transduction vehicle into a target cell if a large number of foreign proteins are packaged per virion. A lentiviral vector, approved for human gene therapy,[1] has been produced by transfecting 293T cells with four plasmids: the gene transfer vector that provides the viral genome packaged into the virion, and three plasmid vectors, each expressing *gag–pol*, *rev* or the vesicular stomatitis virus-G (VSV-G) genome.[2–4] The *gag–pol* expression vector produces Gag and Gag-pol in a ratio of ~20:1 because of the frameshift signal positioned between the *gag* and *pol* open reading frames.[5] Gag ($Pr55^{Gag}$) is a viral structural protein that traffics to the plasma membrane aided by its amino-terminal myristoyl group, and self-oligomerizes at the plasma membrane to form a spherical structure.[6] The expression of Gag alone leads to the production of an enveloped virus-like particle (VLP) of ~100 nm in diameter, consisting of ~5000 Gag molecules.[7]

When the *gag–pol* expression vector is used to produce VLP, both Gag and Gag-pol proteins, a total of 5000 molecules,[7] form the lentiviral nanoparticles in which approximately one-twentieth of the VLP-forming protein is Gag-pol.[5] The VLP produced by the *gag–pol* expression vector undergoes maturation whereby Gag is processed by the protease made from Pol. Gag is cleaved into $p17^{MA}$, $p24^{CA}$ and other smaller fragments. This changes the shape of the VLP core from doughnut shape to bullet shape, as visualized by electron microscopy. Mediated by VSV-G, the mature VLP envelope fuses to the cell membrane more efficiently than the immature VLP.[8] In accordance with this process, if a foreign protein is fused to lentiviral Gag, a large number of foreign proteins should be transduced into mammalian cells. In this work, the lentiviral vector has been engineered to achieve this goal.

By co-transfecting two plasmid vectors, each expressing *gag–pol* or VSV-G, the lentivirus-like nanoparticles (LENA) can be produced with a VSV-G envelope (Figure 1a). These particles undergo maturation, and should be highly competent for promoting fusion of LENA envelope to the cell membrane. The VSV-G-pseudotyped LENA should be capable of releasing viral content into the target cells. We have named this process 'pseudoinfection' because it mimics viral infection, but is not accompanied by integration of the viral genome into chromosomal DNA.

We have previously shown that substitution of the human immunodeficiency virus type 1 (HIV-1) Gag myristoylation signal with the phospholipase C-δ 1 pleckstrin homology (PH) domain, or attachment of heterologous myristoylation signals to the amino-terminus of Gag, increases the production of lentiviral vector.[9,10] In these studies we used the human codon-optimized *gag–pol* to maximize viral protein synthesis. The infectivity of these pseudovirions was comparable with that of the wild-type (WT) counterpart. This is noteworthy because modification of Gag often results in reduction of viral productivity and infectivity.[11,12] It has been reported recently that a protein transduction using murine leukemia virus is achievable by embedding a foreign gene in *gag*. However, the viral productivity and infectivity need to be improved by WT Gag-pol provided in *trans* upon viral production. These data suggest that by fusing a foreign protein to the amino-terminus of Gag and providing a membrane-targeting signal, it is possible to produce a high-titer, uniform, foreign protein-containing LENA without the need to co-transfect the WT Gag-pol expression plasmid. We tested whether the VSV-G-pseudotyped

[1]AIDS Research Center, National Institute of Infectious Diseases, Shinjuku-ku, Tokyo, Japan
Correspondence: Dr J Komano, AIDS Research Center, National Institute of Infectious Diseases, Toyama, 1-23-1, Shinjuku-ku, Tokyo 162-8640, Japan.
E-mail: ajkomano@nih.go.jp
[2]These authors contributed equally to this work.
Received 29 August 2010; revised 2 December 2010; accepted 3 January 2011; published online 31 March 2011

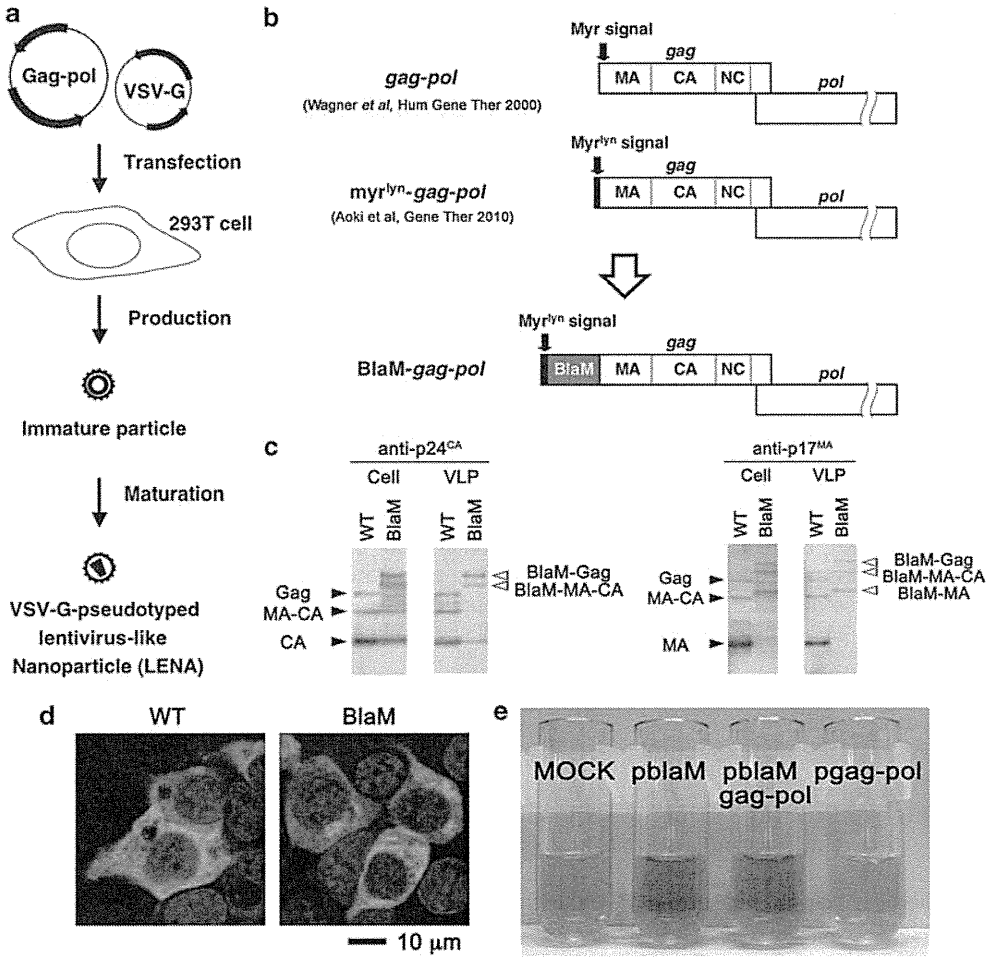

Figure 1 Production of a BlaM-containing LENA pseudotyped with VSV-G. (**a**) Schematic representation of production of VSV-G-pseudotyped LENA. Two plasmids are transfected into 293T cells, and LENA is recovered from the culture supernatant at 48 h post-transfection. The viral protease is activated after the VLP is released from the cell, and it mediates the maturation of the particles. (**b**) The structure of WT *gag–pol*, a mutant bearing the myristoylation signal of *lyn* (myr^{lyn}-*gag-pol*), and *blaM-gag-pol*. Gag is cleaved into p17^{MA} (MA), p24^{CA} (CA), nucleocapsid (NC) and other domains by the viral protease encoded in *pol*. In the myr^{lyn}-*gag-pol* and *blaM-gag-pol* constructs, the Gag translational initiation site and the myristoylation target residues were mutated to leucine and alanine to minimize internal translational initiation and myristoylation. (**c**) Verification of protein expression and VLP production of BlaM-gag-pol construct in 293T cells by western blot analysis using anti-p24^{CA} and anti-p17^{MA} antibodies. Shown are the analyses of cell lysates (Cell) transfected with p*gag-pol* (WT) or p*blaM-gag-pol* (BlaM), and the viral particles (VLP) collected from the culture supernatant of transfected cells. Pr55^{Gag} (~55 kDa, Gag), the Gag proteolytic cleavage intermediate MA–CA (~40 kDa) and the complete proteolytic cleavage product p24^{CA} (~24 kDa, CA) and p17^{MA} (~17 kDa, MA) are indicated by arrowheads. BlaM-Gag, BlaM-MA-CA and BlaM-MA have higher molecular weights because of the attachment of BlaM (~30 kDa) to the MA domain. (**d**) Immunofluorescence assay showing the distribution of WT Gag (WT) or BlaM-Gag (BlaM) in 293T cells transfected with p*gag-pol* or p*blaM-gag-pol*. Green and blue represent the anti-p24^{CA} monoclonal antibody-stained signal and the Hoechst 33258-stained nucleus, respectively. Magnification ×400; scale bar, 10 μm. (**e**) BlaM enzyme activity was tested by nitrocefin. Lysates from 293T cells transfected with p*blaM*, p*blaM-gag-pol*, *or* p*gag-pol* or untransfected cells (MOCK) were incubated with nitrocefin for 30 min at 37 °C.

LENA could serve as a protein transduction vehicle for mammalian cells using β-lactamase (BlaM) as a reporter.

RESULTS AND DISCUSSION

BlaM was chosen as reporter molecule because mammalian cells do not have BlaM activity. Also, a cell-membrane-permeable BlaM substrate is available, which can distinguish LENA content release from cellular endocytosis of LENA that can occur without membrane fusion.[13] *BlaM* was fused to the amino-terminus of *gag–pol*, and the *lyn* myristoylation signal was attached to the amino-terminus of *BlaM* (*BlaM-gag-pol*; Figure 1b). The codon usage of *gag–pol* has been human codon optimized, but bearing the natural −1 frameshift signal at the *gag–pol* junction.[14] Thus, the vector provides the natural Gag to Gag-pol ratio. The BlaM-gag-pol protein was produced in 293T cells as expected (Figure 1c). The *BlaM* construct produced VLP from the transfected cells, although the efficiency was less than with WT *gag–pol* (Figure 1c). The processing efficacy of Gag in BlaM VLP was less efficient compared with the WT as highlighted by the absence of free matrix domain (MA) signal in BlaM VLP, which was because of the lack of HIV-1 protease recognition motif between BlaM and MA (right panel, Figure 1c). In 293T cells transiently transfected with this plasmid, the BlaM-gag-pol fusion protein distribution was similar to that of the WT, although with some aggregation in the cytoplasm (Figure 1d). The BlaM-gag-pol fusion protein retained enzyme activity as demonstrated by its reaction with the BlaM substrate nitrocefin, which changed from a straw color to brown when incubated with

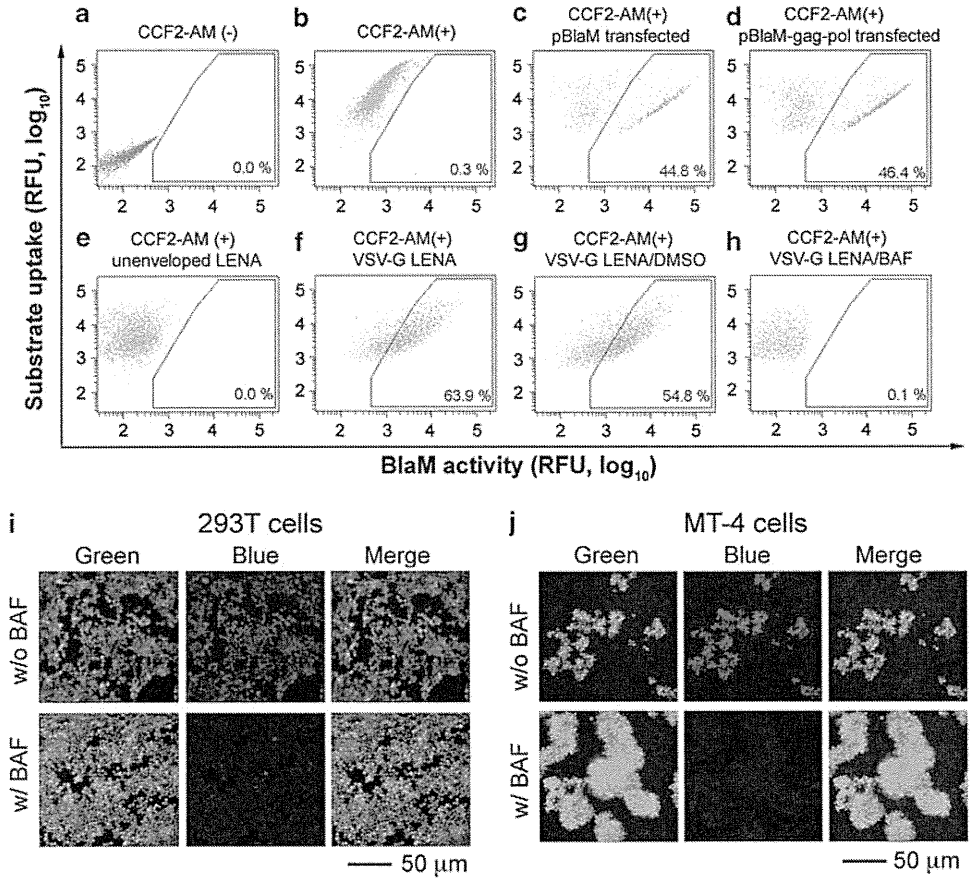

Figure 2 Flow cytometric analysis to measure the BlaM transduction into 293T cells by VSV-G-pseudotyped BlaM-LENA. The 293T cells were grown in 24-well plates and either transfected or pseudoinfected with LENA preparations. (**a**) Unstained 293T cells. (**b**) 293T cells loaded with CCF2-AM. (**c**, **d**) 293T cells were transfected with pBlaM (**c**) or pBlaM-gag-pol (**d**), and loaded with CCF2-AM at 48 h post-transfection before the flow cytometric analysis. (**e–h**) 293T cells were exposed to unenveloped BlaM-LENA (**e**) or VSV-G-pseudotyped BlaM-LENA (**f–h**). Cells were loaded with CCF2-AM at 2 h post-LENA exposure. (**g**, **h**) The VSV-G-dependent BlaM transduction was verified by exposing 293T cells with VSV-G-pseudotyped BlaM-LENA in the presence of bafilomycin A1 (BAF) at a concentration of 10 μg ml^{-1} (**h**). Dimethylsulfoxide (DMSO) was used as a control (**g**). The percentage of the gated population is noted in each panel. The *x* axis represents the blue fluorescence, reflecting the BlaM activity (relative fluorescent unit (RFU)). The *y* axis represents the green fluorescence, reflecting the substrate loading onto the cells. (**i**, **j**) Microscopic detection of BlaM transduction in 293T cells (**i**) or MT-4 cells (**j**) by VSV-G-pseudotyped BlaM-LENA. Cells were exposed to BlaM-LENA for 3 h, and loaded with CCF2-AM overnight at room temperature in the presence (10 μg ml^{-1}) or absence of BAF (w/BAF or w/o BAF, respectively). The bar represents 50 μm, magnification ×200.

lysates from 293T cells transfected with the BlaM-gag-pol expression vector (Figure 1e). The BlaM enzyme activity of BlaM-gag-pol was indistinguishable from that of WT BlaM (Figure 1e). BlaM enzyme activity was not detected in MOCK or p*gag-pol*-transfected cell lysates (Figure 1e).

Protein transduction into 293T cells was conducted by exposing target cells to VSV-G-pseudotyped BlaM-LENA, which mimics viral infection. The success of BlaM transduction into the target cell cytoplasm was judged by using the cytoplasm-retained BlaM substrate, CCF2-AM, which yields blue fluorescence upon cleavage by BlaM enzyme activity.

The 293T cells emitted green fluorescence when they were loaded with CCF2-AM (Figure 2, compare a vs b). When 293T cells were transfected with expression vectors for BlaM or the BlaM-gag-pol, substrate cleavage, as demonstrated by a shift to blue fluorescence, was detected in a discrete population of cells, representing a transfection efficiency of ~45% (Figures 2c and d). These data suggest that transduced BlaM-gag-pol has BlaM activity, consistent with the results of the nitrocefin assay (Figure 1e). When BlaM was transduced into 293T cells by VSV-G-pseudotyped BlaM-LENA, a significant shift from green to blue fluorescence was detected (63.9%, Figure 2f). The rightward shift of the signal along the *x* axis suggests that almost all the cells were transduced with BlaM by BlaM-LENA. BlaM transduction was dependent on VSV-G function as CCF2-AM cleavage was not detected by LENA lacking VSV-G (Figure 2e), and BlaM transduction was inhibited by bafilomycin A1 that blocks VSV-G-mediated membrane fusion (Figure 2, compare g vs h). The catalytic activity was visualized under the fluorescent microscopy. In agreement with the flow cytometric analysis, almost all the substrate-loaded 293T cells exposed to BlaM-LENA became blue fluorescent in experimental conditions comparable with the above experiments, and the catalytic activity was not detected when cells were treated with bafilomycin A1 (Figure 2i). The blue fluorescence was detected homogenously in the cell cytoplasm (Figure 2i). These data were reproduced in human T-cell line MT-4 (Figure 2j). Considering the critical dependence to VSV-G, it is highly unlikely that the BlaM activity was derived from the residual DNA/lipid mixture in the LENA preparation. The BlaM-transducing unit into 293T cells was ~$0.8 \pm 0.01 \times 10^9$ ml^{-1} as

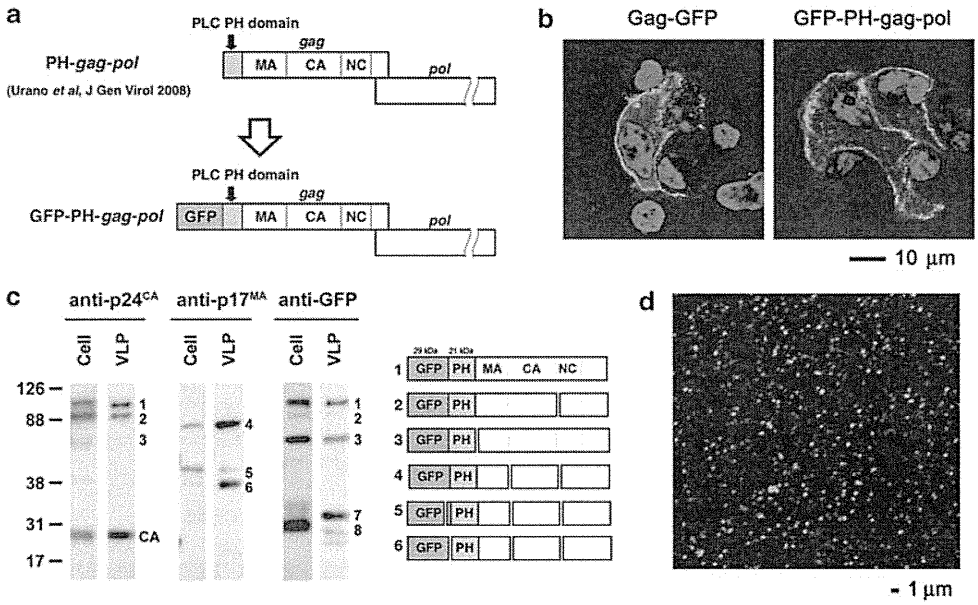

Figure 3 Production of a GFP-containing lentivirus-like nanoparticle for physical counting. (**a**) The structure of PH-*gag-pol* and GFP-PH-*gag-pol*. (**b**) The distribution of Gag-GFP and GFP-PH-gag-pol in transiently transfected 293T cells examined by confocal microscopy. The images were taken at 24 h post-transfection. The bar represents 10 μm, magnification ×630. (**c**) Verification of protein expression and VLP production of GFP-PH-gag-pol construct in 293T cells by western blot analysis using anti-$p24^{CA}$, anti-$p17^{MA}$ and anti-GFP antibodies. Shown are the analyses of cell lysates (Cell) transfected with pGFP-PH-*gag-pol* and the viral particles (VLP) collected from the culture supernatant of transfected cells. The numbers represent the proteolytic products as illustrated in the right panel estimated from the western blot analysis. (**d**) Confocal image of the GFP-PH-LENA on the slide glass. The bar represents 1 μm, magnification ×630.

estimated by the BlaM-LENA serial dilution (data not shown). Thus, 293T cells were exposed to ~1000-fold excess of BlaM-LENA.

We constructed GFP-PH-LENA to visualize the LENA particles (Figure 3a). In this construct, the PH domain from phospholipase C-δ 1 functions as the membrane targeting motif.[9,10] The GFP-PH-gag-pol was distributed at cell periphery, similar to Gag-GFP (Figure 3b). The VLP production by GFP-PH-gag-pol was verified in western blot analysis (Figure 3c). According to the estimated molecular weight of protease-mediated cleavage products, we speculate the possible protease recognition sites within green fluorescent protein (GFP), GFP–PH junction and PH–MA junction, although we did not intentionally reconstitute the HIV-1 protease recognition sites in these positions (Figure 3c). The GFP-encapsidated LENA preparations were spotted onto the poly-L-lysine-coated slide glass, and the captured LENA was imaged by the confocal microscopy. By counting the green fluorescent dot signals per unit area, we estimated the number of GFP-PH-LENA particles as $1.4 \pm 0.2 \times 10^9$ ml^{-1} (Figure 3d), which was similar to the BlaM-transduction unit of VSV-G-pseudotyped BlaM-LENA.

To test whether the lentivirus vector used to produce BlaM-LENA retained any viral infectivity, a lentivirus vector was produced carrying the luciferase gene, using the four plasmid system[9,10] with the BlaM-gag-pol construct, and then viral infectivity was assessed. Gene transduction by this lentiviral vector was undetectable. These data indicate that transfer to target cells by BlaM-LENA of an expressed, endogenous retroviral element from 293T cells is unlikely to occur. These data show that a protein transduction system based on LENA would have an extra level of safety compared with the protein transduction system based on a retroviral vector system.[11]

Protein transduction in a broad sense, referring to the transport of protein across the cell membrane, is a useful technique in experimental molecular biology. It does not require *de novo* transcription and translation, and the transferred protein functions immediately after the transduction. Proteins, however, do not easily pass through the plasma membrane. Historically, microinjection, electroporation and cell-permeable peptide motifs were used to introduce proteins into cells.[15–17] These methods, however, demand a highly purified protein, technical skill or specialized, costly equipment. Also, variable results have been obtained using different proteins and target cells. The need of a highly purified protein applies to protein lipofection to yield the reproducible results. A convenient, fast, highly efficient and reproducible protein transduction method has so far remained undeveloped. Such a technique would greatly help the generation of safe, induced pluripotent stem cells. LENA production is as straightforward as co-transfecting two plasmids into 293T cells without *trans*-complementing the WT *gag–pol* expression vector, and furthermore the therapeutic protein is protected from plasma proteases by a lipid bilayer. The target cell tropism can be controlled by well-established viral pseudotype techniques. Using LENA, a substantial number of protein molecules can be packaged into the nanoparticles, and the transduction procedure is as easy as exposing mammalian cells with LENA. There is no need to prepare highly purified proteins for the LENA system. Also, target proteins are post-translationally modified in human cells, which should be better than the protein modification in non-human organisms. It should also be possible to increase the amount of protein that can be delivered into cells by concentrating the LENA preparation. Physical counting of GFP-encapsidated LENA shows that a high-titer LENA preparation was casually produced. In this study, we did not introduce protease recognition sites into myristoylation signal-BlaM or -BlaM-MA junctions. By doing so, we would have possibly liberated the foreign protein from the precursor. This could result in infectious LENA particles as the free MA is in part important for the viral infectivity.[9]

Currently, few approaches are available for the incorporation of a foreign protein into retro- or lenti-viral VLP. The protein of interest

can be fused to the C-terminus of Gag or inserted into the middle of the Gag protein (for example, between the MA and CA).[11,12] Foreign protein fusion to the C-terminus of Gag would destroy the frameshift signal required to produce Gag-pol. Thus, Pol would no longer be produced. To maintain efficient pseudoinfection, the *gag–pol* expression vector must be provided in *trans* when the VLP is produced. The latter approach often results in reduced VLP yield. Thus, again, to increase the VLP yield, the *gag–pol* expression vector has to be co-transfected with the plasmid encoding Gag fused to the foreign protein. Co-transfection of the *gag–pol* expression vector is likely to reduce the amount of foreign protein per VLP, and lower its uniformity. It is, therefore, desirable not to co-transfect with the WT *gag–pol* expression plasmid. Alternatively, Vpr can be used to incorporate foreign proteins into lentiviral particles.[18] Only a few dozen protein molecules, however, are packed per particle, rendering this approach of little use in protein transduction. In summary, fusion of a foreign protein to the N-terminus of Gag has the advantages of producing uniform, high-titer and membrane fusion-competent VLP without *trans*-complementation by WT Gag-pol.

The disadvantages of the LENA system are the susceptibility of foreign proteins to viral protease and the restriction in the molecular sizes of foreign proteins. We have succeeded in generating Gag-LacZ VLP, suggesting that the production of LENA carrying a foreign protein with a molecular weight of ~100 kDa is feasible. The yield, however, of LENA gradually decreases as the molecular weight of the foreign protein increases. We did not detect proteolytic cleavage of BlaM by viral protease in LENA particles; however, when we tested the transcriptional regulator of HTLV-1 (human T-cell leukemia virus type 1), Tax, it was degraded by viral protease. To overcome these potential disadvantages, it is worth considering the use of only the minimal functional domain of a foreign protein and the destruction of potential protease recognition sites in the foreign protein without losing its function.

Lentiviral vectors have been approved for human gene therapy.[1] LENA does not contain a viral genome, and is unlikely to support the transfer of endogenous retrovirus-like elements; thus, the cellular genome is not threatened by LENA-mediated protein transduction. Thus, a major safety concern associated with retroviral or lentiviral vectors is alleviated, making LENA applicable for *in vivo* studies. Retroviral vectors are often used for induced pluripotent stem cell genesis.[19] However, they can damage the cellular genome, and transduced gene expression is difficult to shut off, which can lead to malignant transformation of induced pluripotent stem cells. To overcome this problem, a transient and efficient protein transduction method is needed. We believe that LENA addresses these issues. Altogether, our system has many advantages over currently available protein transduction protocols, suggesting that it should be considered for basic and clinical applications.

MATERIALS AND METHODS

Plasmids

The following oligonucleotides were annealed, and cloned into the *AfeI–AgeI* sites of pEGFP-C2 (Clontech, Palo Alto, CA, USA) to generate the p*lyn*MyEGFP-C2: 5′-GCTACCGGACTCAGATCTCGAGCTCAAGCTTCGAATTGC CACCATGGGATGTATTAAATCAAAAAGGAAAGACGATCCA-3′ and 5′-CCG GTGGATCGTCTTTCCTTTTTGATTTAATACATCCCATGGTGGCAATTCGA AGCTTGAGCTCGAGATCTGAGTCCGGTAGC-3′. The *SnaBI–EcoRI* fragment from p*lyn*MyEGFP-C2 was cloned into the corresponding sites of pPH-*gag-pol*,[9] generating p*lyn*MyGFP-*gag-pol*. The β-lactamase gene from pUC19 was amplified by the following primers: 5′-ACCGGTCAATCCAGAAACGCTGGTG AAAG-3′ and 5′-CAATTGCCAATGCTTAATCAGTGAGGC-3′. The *AgeI–MfeI* fragment of the PCR fragment was cloned into the *AgeI–EcoRI* sites of p*lyn*MyGFP-*gag-pol*, generating the p*blaM-gag-pol*. The expression vector for VSV-G was described previously.[20] The original codon-optimized HIV-1 *gag–pol* expression vector was described previously.[14] The Gag-GFP expression vector was described previously.[10] The pGFP-PH-*gag-pol* was constructed by inserting the *NdeI–PshAI* fragment from pEGFP-PLCd1 PH[21] into the corresponding sites of pPH-*gag-pol*.[9] pcDNA3 was obtained from Invitrogen (Tokyo, Japan).

Cells and transfection

The 293T cells, obtained from Invitrogen as 293FT cells (Invitrogen), were maintained in RPMI-1640 medium (Sigma, St Louis, MA, USA) supplemented with 10% fetal bovine serum (Japan Bioserum, Tokyo, Japan), 50 U ml^{-1} penicillin and 50 μg ml^{-1} streptomycin (Invitrogen), at 37 °C in a humidified 5% CO_2 atmosphere. Cells were transfected with DNA using Lipofectamine 2000 according to the manufacturer's protocol (Invitrogen), or calcium phosphate precipitation. To produce VSV-G-pseudotyped BlaM-LENA, equal amounts of pVSV-G and p*blaM-gag-pol* were transfected into 293T cells. Unenveloped BlaM-LENA was produced using pcDNA3 in place of pVSV-G.

Immunological detection

The detection of viral gene products by western blot analysis was performed as described previously,[22] except that the anti-p24^{CA} monoclonal antibody clone 183-H12-5C and the anti-p17^{MA} rabbit antiserum (NIH AIDS Research and Reference Reagent Program) were used. The immunofluorescent analysis was performed as described previously,[22] except that cells were fixed at 24 h post-transfection, and the following reagents were used: anti-p24^{CA} monoclonal antibody (clone 183-H12-5C), anti-mouse antibody conjugated with biotin (Invitrogen) and streptavidin conjugated with Alexa488 (Invitrogen).

Microscopy

Cells and GFP-encapsidated LENA were imaged by confocal fluorescence microscopy (LSM510 Meta 40× NA 1.4 lens; Carl Zeiss MicroImaging Inc., Tokyo, Japan).

Colorimetric detection of BlaM activity

Transfected 293T cells grown in 6 cm dishes were lysed in 500 μl of buffer A (10 mM HEPES, 1.5 mM $MgCl_2$, 10 mM KCl and 0.05% IGEPAL CA-630), and then 1 μl of nitrocefin (10 μg ml^{-1}; Calbiochem, San Diego, CA, USA) was added to the cell lysate. The mixture was incubated for 20 min at 37 °C.

Protein transduction

The pseudoinfection was performed as infecting cells with retroviral vectors[20] by incubating ~1×10^6 cells with 1 ml LENA-containing culture medium at 37 °C for 1–3 h in the presence of dextran (final concentration 16.25 μg ml^{-1}; DEAE-Dextran chloride, molecular weight ~500 kDa; ICN Biomedicals Inc., Aurora, OH, USA). The cells were assayed by flow cytometry or fluorescent microscopy after the LENA exposure. Bafilomycin A1 was purchased from Sigma.

Fluorescent detection of BlaM activity

A fluorescence-activated cell sorter Aria (Becton Dickinson, San Jose, CA, USA) was used to detect the CCF2-AM (Invitrogen) signals from 293T cells. A violet 407 nm laser was used for fluorescence activation, and BP450/40 nm and LP502 in conjunction with BP530/30 filters were used for the fluorescent signal detection of cleaved and uncleaved substrates, respectively. The CCF2-AM signals from 293T and MT-4 cells were imaged by Biorevo (BZ-9000, Keyence, Osaka, Japan) using the blue filter set (excitation, band pass filters 377/50 nm wavelength; emission, band pass 447/60 nm wavelength; dichroic mirror, 409 nm wavelength) and the green filter set (excitation, band pass filters 377/50 nm wavelength; emission, band pass 520/35 nm wavelength; dichroic mirror, 495 nm wavelength).

CONFLICT OF INTEREST

The authors declare no conflict of interest.

ACKNOWLEDGEMENTS

This work was supported by the Japan Health Science Foundation, the Japanese Ministry of Health, Labor, and Welfare (H18-AIDS-W-003 to JK) and the Japanese Ministry of Education, Culture, Sports, Science and Technology (18689014 and 18659136 to JK).

1 MacGregor RR. Clinical protocol. A phase 1 open-label clinical trial of the safety and tolerability of single escalating doses of autologous CD4 T cells transduced with VRX496 in HIV-positive subjects. *Hum Gene Ther* 2001; **12**: 2028–2029.
2 Cockrell AS, Kafri T. Gene delivery by lentivirus vectors. *Mol Biotechnol* 2007; **36**: 184–204.
3 McCart JA, Bartlett DI. Lentiviral Vectors. In: Templeton NS (ed.). *Gene and Cell Therapy: Therapeutic Mechanisms and Strategies*, 3rd edn. CRC Press: Carrollton, 2008, pp 245–262.
4 Lundberg C, Björklund T, Carlsson T, Jakobsson J, Hantraye P, Déglon N *et al.* Applications of lentiviral vectors for biology and gene therapy of neurological disorders. *Curr Gene Ther* 2008; **8**: 461–473.
5 Jacks T, Power MD, Masiarz FR, Luciw PA, Barr PJ, Varmus HE. Characterization of ribosomal frameshifting in HIV-1 gag-pol expression. *Nature* 1988; **331**: 280–283.
6 Klein KC, Reed JC, Lingappa JR. Intracellular destinies: degradation, targeting, assembly, and endocytosis of HIV Gag. *AIDS Rev* 2007; **9**: 150–161.
7 Briggs JA, Simon MN, Gross I, Kräusslich HG, Fuller SD, Vogt VM *et al.* The stoichiometry of Gag protein in HIV-1. *Nat Struct Mol Biol* 2004; **11**: 672–675.
8 Wyma DJ, Jiang J, Shi J, Zhou J, Lineberger JE, Miller MD *et al.* Coupling of human immunodeficiency virus type 1 fusion to virion maturation: a novel role of the gp41 cytoplasmic tail. *J Virol* 2004; **78**: 3429–3435.
9 Urano E, Aoki T, Futahashi Y, Murakami T, Morikawa Y, Yamamoto N *et al.* Substitution of the myristoylation signal of human immunodeficiency virus type 1 Pr55Gag with the phospholipase C-delta1 pleckstrin homology domain results in infectious pseudovirion production. *J Gen Virol* 2008; **89**: 3144–3149.
10 Aoki T, Shimizu S, Urano E, Futahashi Y, Hamatake M, Tamamura H *et al.* Improvement of lentiviral vector-mediated gene transduction by genetic engineering of the structural protein Pr55(Gag). *Gene Therapy* 2010; **17**: 1124–1133.
11 Voelkel C, Galla M, Maetzig T, Warlich E, Kuehle J, Zychlinski D *et al.* Protein transduction from retroviral Gag precursors. *Proc Natl Acad Sci USA* 2010; **107**: 7805–7810.
12 Hubner W, Chen P, Del Portillo A, Liu Y, Gordon RE, Chen BK. Sequence of human immunodeficiency virus type 1 (HIV-1) Gag localization and oligomerization monitored with live confocal imaging of a replication-competent, fluorescently tagged HIV-1. *J Virol* 2007; **81**: 12596–12607.
13 Campbell RE. Realization of beta-lactamase as a versatile fluorogenic reporter. *Trends Biotechnol* 2004; **22**: 208–211.
14 Wagner R, Graf M, Bieler K, Wolf H, Grunwald T, Foley P *et al.* Rev-independent expression of synthetic gag-pol genes of human immunodeficiency virus type 1 and simian immunodeficiency virus: implications for the safety of lentiviral vectors. *Hum Gene Ther* 2000; **11**: 2403–2413.
15 Ulett GA, Han S, Han JS. Electroacupuncture: mechanisms and clinical application. *Biol Psychiatry* 1998; **44**: 129–138.
16 Ford KG, Souberbielle BE, Darling D, Farzaneh F. Protein transduction: an alternative to genetic intervention? *Gene Therapy* 2001; **8**: 1–4.
17 Zhang Y, Yu LC. Microinjection as a tool of mechanical delivery. *Curr Opin Biotechnol* 2008; **19**: 506–510.
18 Cavrois M, De Noronha C, Greene WC. A sensitive and specific enzyme-based assay detecting HIV-1 virion fusion in primary T lymphocytes. *Nat Biotechnol* 2002; **20**: 1151–1154.
19 Yamanaka S, Blau HM. Nuclear reprogramming to a pluripotent state by three approaches. *Nature* 2010; **465**: 704–712.
20 Komano J, Miyauchi K, Matsuda Z, Yamamoto N. Inhibiting the Arp2/3 complex limits infection of both intracellular mature vaccinia virus and primate lentiviruses. *Mol Biol Cell* 2004; **15**: 5197–5207.
21 Stauffer TP, Ahn S, Meyer T. Receptor-induced transient reduction in plasma membrane PtdIns(4,5)P2 concentration monitored in living cells. *Curr Biol* 1998; **8**: 343–346.
22 Miyauchi K, Komano J, Yokomaku Y, Sugiura W, Yamamoto N, Matsuda Z. Role of the specific amino acid sequence of the membrane-spanning domain of human immunodeficiency virus type 1 in membrane fusion. *J Virol* 2005; **79**: 4720–4729.

Cancer Science
The official journal of the Japanese Cancer Association JCA

Cytokine signatures of transformed B cells with distinct Epstein–Barr virus latencies as a potential diagnostic tool for B cell lymphoma

Kosuke Miyauchi,[1] Emiko Urano,[1] Hironori Yoshiyama[2] and Jun Komano[1,3]

[1]AIDS Research Center, National Institute of Infectious Diseases, Tokyo; [2]Research Center for Infection-associated Cancer, Institute for Genetic Medicine, Hokkaido University, Sapporo, Japan

(Received November 2, 2010/Revised March 4, 2011/Accepted March 7, 2011/Accepted manuscript online March 10, 2011/Article first published online March 31, 2011)

Immunocompromised individuals, including those infected with human immunodeficiency virus (HIV), are at increased risk of Epstein–Barr virus (EBV)-associated aggressive B cell malignancies such as Burkitt's lymphoma (BL) or diffuse large B cell lymphoma (DLBCL). Differential diagnosis of these lymphomas requires histopathological, immunohistochemical and cytogenetic assessments. Rapid, less invasive approaches to the diagnosis of EBV-associated B cell lymphomas are needed. Here, high-throughput cytokine profiling of BL cell lines and EBV-transformed B lymphoblastoid cell lines (B-LCL), representing DLBCL, was carried out. By monitoring the production of 42 different cytokines, unique cytokine signatures were identified for BL and B-LCL/DLBCL. The BL cells produced interleukin (IL)-10, 10 kDa interferon gamma-induced protein (IP-10)/CXCL10, macrophage-derived chemokine (MDC)/CCL22, macrophage inflammatory protein (MIP)-1α/CCL3 and MIP-1β/CCL4. In addition to these five cytokines, the cytokine signature of B-LCL/DLBCL cells included IL-8/CXCL8, IL-13, platelet-derived growth factor (PDGF)-AA, and regulated upon activation, normal T cell expressed and secreted (RANTES)/CCL5. Epstein–Barr virus latency was responsible for the increased production of IL-10, MDC/CCL22 and MIP-1α/CCL3 in BL cells, suggesting that EBV-mediated BL-genesis involves these three cytokines. These results suggest that high-throughput cytokine profiling might be a valuable tool for the differential diagnosis and might deepen our understanding of the pathogenesis of EBV-associated B cell malignancies. (*Cancer Sci* 2011; 102: 1236–1241)

Epstein–Barr virus (EBV) is a human gamma herpes virus that has been linked to the development of Burkitt's lymphoma (BL) and diffuse large B cell lymphoma (DLBCL) in immunocompromised individuals, including those with acquired immunodeficiency syndrome (AIDS).[1–4] B lymphoblastoid cell lines (B-LCL), which arise from the EBV-transformed peripheral B cells, serve as a model of EBV-associated DLBCL.[5] The EBV-positive BL and EBV-transformed B-LCL and some BL cell lines produce an array of cytokines at varying levels, including interleukin (IL)-6, IL-8/CXCL8, IL-10, monocyte chemoattractant protein (MCP)-1/CCL2, macrophage-derived chemokine (MDC)/CCL22, macrophage inflammatory protein (MIP)-1α/CCL3, MIP-1β/CCL4, regulated upon activation, normal T cell expressed and secreted (RANTES)/CCL5, thymus and activation-regulated chemokine (TARC)/CCL17, tumor necrosis factor (TNF)α and TNFβ.[6–12] Certain cytokines can be detected in the sera of individuals with EBV-associated malignancies, which suggests an active role for these and perhaps other cytokines in disease pathogenesis.[7,13,14] Certain cytokines, such as IL-6 or IL-10, have been proposed as diagnostic and/or prognostic markers of EBV-associated B cell malignancies.[7,9,15] However, these cytokines are not widely used clinically primarily due to their lack of specificity and sensitivity. One way to demonstrate the utility of cytokine profiles as a specific diagnostic marker is to analyze a number of different cytokines in parallel.

Epstein–Barr virus establishes latent infection in the infected cells in which only a limited number of viral latency-associated genes are expressed, including EBNA and LMP. In this latency, EBV does not produce progeny viruses actively. There are three types of EBV latency, type I, II and III,[5] each of which is associated with the expression of different sets of latent genes. In BL cells, EBV type I latency *in vivo* involves the expression of only a few viral latent genes, including EBNA1, BARF0, EBER.[5] In DLBCL, EBV establishes type III latency, in which all of the viral latent genes are expressed, including EBNA2, EBNA3, EBNA-LP, LMP, in addition to the type I latency associated genes.[5] Cytokines produced by EBV-infected B cells during type III latency are well documented because the genes expressed during type III latency, including LMP-1, are strong inducers of cytokine production. In contrast, other than IL-10, the cytokines produced by BL cells in type I latency are less well characterized.

Historically, the dysregulation of cytokine production by latent EBV infection has been studied by comparing the cytokine profiles of EBV-positive and EBV-negative BL cell lines, or by monitoring cytokine production of primary B cells after EBV infection, or EBV-negative BL cell lines transfected with EBV genes.[4,11,16,17] However, there are several caveats to these methods. Comparisons using cell lines might not be sensitive enough to detect correlations between EBV status and cytokine production because baseline cytokine production varies among cell lines. The analysis of cytokine dysregulation induced by type I latency has been problematic because EBV infection of primary B cells and EBV-negative BL cells *in vitro* results in type III latency. Finally, transfection protocols typically use cells that are non-B cell in origin, or are limited to a few EBV-negative B cell lines, and the results from such experiments might not be relevant to cytokine production by BL cells with type I EBV latency.

To achieve better sensitivity and accuracy in detecting altered cytokine production associated with latent EBV infection, especially type I latency, the preferred method is a comparison of EBV-positive cells with the EBV negative from the same origin. Recently, EBV-negative cell clones were successfully isolated from the EBV-positive BL cell lines Akata, Daudi and Mutu.[18,19] These cells have previously been used as a model system for elucidating the oncogenic role of EBV in type I BL cells.[20–22] Dysregulation of cytokine production induced by type I EBV latency should be possible through systematic cytokine profiling of these EBV-positive and EBV-negative BL cells.

[3]To whom correspondence should be addressed. E-mail: ajkomano@nih.go.jp

doi: 10.1111/j.1349-7006.2011.01924.x

In the current study, we assessed the production of 42 cytokines by EBV-positive type I BL cell lines and their corresponding EBV-negative counterparts at the protein level using a high-throughput microbead-based system. We also analyzed cytokine production of B-LCL, a BL-like cell line, as well as T lymphoblastoid cell lines and primary blood mononuclear cells (PBMC). We identified cytokine signatures that are characteristic of type I BL and B-LCL that might be useful in the differential diagnosis and prognosis of EBV-associated B cell malignancies.

Materials and Methods

Cells. Cells were maintained in RPMI 1640 medium (Sigma, St. Louis, MA, USA) supplemented with 10% fetal bovine serum (Japan Bioserum, Tokyo, Japan), 50 U/mL penicillin and 50 μg/mL streptomycin (Invitrogen, Tokyo, Japan) at 37°C in a humidified 5% CO_2 atmosphere. The following cells lines were used: Akata, a Japanese EBV-positive BL cell line (non-AIDS related);[23] Daudi, an African EBV-positive BL cell line (non-AIDS related);[6] BJAB, an African EBV-negative Burkitt-like lymphoma cell line that lacks the c-myc translocation (non-AIDS related);[24] and Mutu, an African EBV-positive BL cell line.[25] The B-LCL were established by infecting healthy donor-derived B cells with EBV of Akata[26] or B95-8 origin.[27] B95-8-derived recombinant EBV carrying a G418-resistance gene has been developed by Shimizu *et al.*[28] as Akata virus. The B-LCL were generated as oligoclonal pools. The CEM, Jurkat and MOLT-4 cell lines were derived from acute T cell lymphoblastic leukemias. MT-4 is a T cell line transformed with human T-cell lymphotropic virus-1 (HTLV-1).[29] An epithelial cell line MKN28 is derived from well-differentiated tubular adenocarcinoma,[30] and the recombinant Akata[28] was used to convert MKN28.[31]

Cytokine assay. Cytokine assays were carried out using a human cytokine/chemokine kit (#MPXHCYTO60KPMX42; Millipore, Tokyo, Japan). Tissue culture supernatants were collected 3–4 days post-cultivation when the cell density was approximately 4–7.5 × 10^5 cells/mL. Signals were detected using a Luminex 200 system (Luminex, Austin, TX, USA) operated with XPONENT 3.1 software (Luminex).

Results

Cytokine production profile of BL cells during different types of EBV latency. We monitored the production of 42 cytokines by three type I BL cell lines (Akata, Daudi and Mutu) and their virus-negative counterparts. The data are summarized in Figure 1 and color-coded according to cytokine concentration (Fig. 1). There were five cytokines that were common to all type I BL cell lines: IL-10, IP-10/CXCL10, MDC/CCL22, MIP-1α/CCL3 and MIP-1β/CCL4, albeit at varying levels (Table 1).

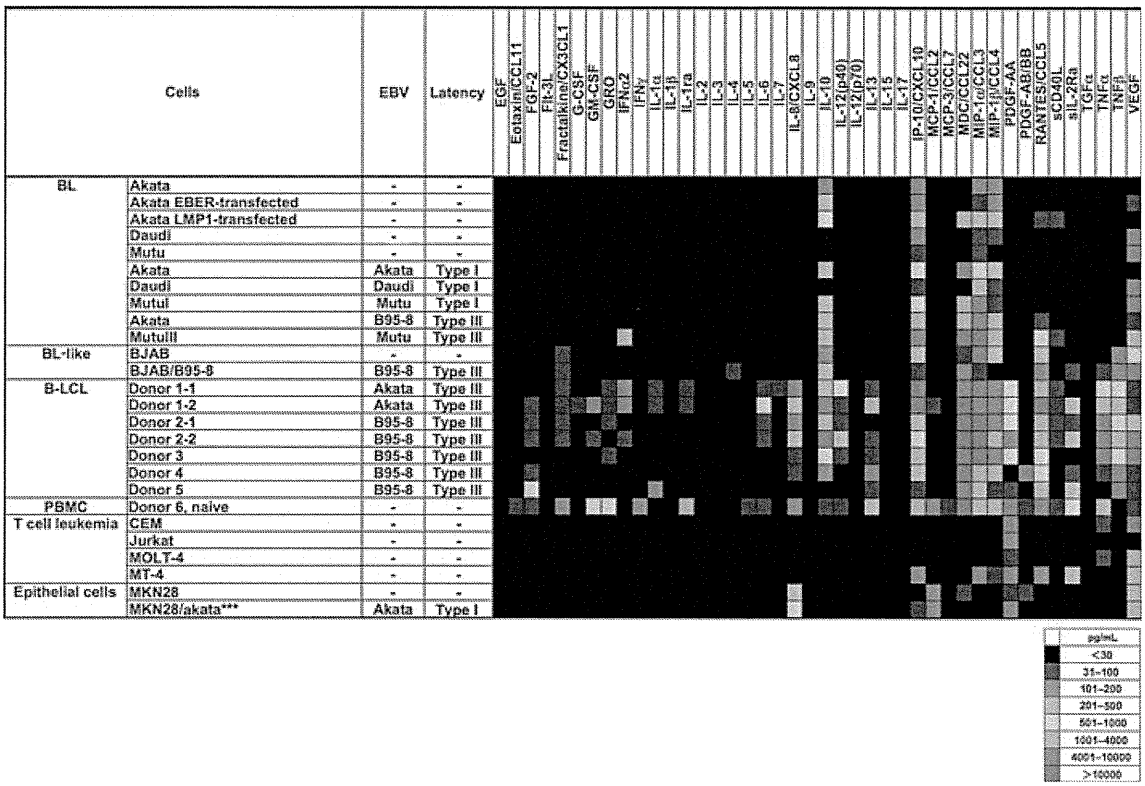

Fig. 1. Cytokine production profiles of various lymphoid cells. To compare cytokine production levels, the data were color-coded according to the expression level, as indicated in the legend. Data represent the average of two independent experiments for Epstein–Barr virus (EBV)-negative Akata and B lymphoblastoid cell line (B-LCL) donor 4. Two independent oligoclonal pools were assayed for B-LCL donors 1 and 2. For Akata/B95-8, a recombinant B95-8 virus containing the G418-resistance gene inserted into the viral TK gene locus was used. For B-LCL/Akata, a recombinant Akata virus containing the G418-resistance gene and a green fluorescence protein (GFP) expression cassette inserted into the viral TK gene locus was used. For MKN28/Akata, a recombinant Akata virus containing the G418-resistance gene inserted into the viral TK gene locus was used. In type I EBV latency, EBNA1, BARF0, and EBER are expressed. In type III EBV latency, all of the latency-associated EBV genes are expressed, including EBNA1, EBNA2, EBNA3, EBNA-LP, EBER, BARF0, and LMP. BL, Burkitt's lymphoma; EGF, epidermal growth factor; FGF, fibroblast growth factor; G-CSF, granulocyte colony-stimulating factor; GM-CSF, granulocyte–macrophage colony-stimulating factor; GRO, growth-related oncogene; IFN, interferon; IL, interleukin; MCP, monocyte chemoattractant protein; MDC, macrophage-derived chemokine; MIP, macrophage inflammatory protein; PDGF, platelet-derived growth factor; RANTES, regulated upon activation, normal T cell expressed and secreted; TGF, transforming growth factor; TNF, tumor necrosis factor; VEGF, vascular endothelial growth factor.

Table 1. Summary of cytokines characteristic to transformed B cells with distinct EBV latency

Status	Cytokines
BL signature cytokines	IL-10, IP-10/CXCL10, MIP-1a/CCL3, MIP-1b/CCL4
Upregulated in BL cells by type I EBV latency	IL-10, MDC/CL22, MIP-1a/CCL3
B-LCL/DLBCL signature cytokines	IL-8/CXCL8, IL-10, IL-13, IP-10/CXCL10, MIP-1a/CCL3, MIP-1b/CCL4, PDGF-AA, RANTES/CCL5

BL, Burkitt's lymphoma; B-LCL, B lymphoblastoid cell lines; DLBCL, diffuse large B cell lymphoma; EBV, Epstein–Barr virus.

This suggested that these cytokines might be involved in BL pathogenesis and that this cytokine signature might be characteristic of type I EBV latency in BL (Fig. 1). To investigate whether this pattern of cytokine production was specifically induced by EBV, we compared the types and concentrations of cytokines produced by type I BL cells with their corresponding EBV-negative counterparts (Fig. 2). The color-coded scale in Figure 1 was sufficient to represent overall trends but was not suitable for analyzing changes in cytokine concentrations. Thus, a new color-coded scale was applied to analyze the magnitude of the differences in cytokine concentrations between EBV-positive and EBV-negative cells in more detail. The levels of IL-10, MDC/CCL22 and MIP-1α/CCL3 were 11.9-, 185.1- and 2.4-fold higher, respectively (average values for all three cell lines), in type I BL cells than in their EBV-negative counterparts (Fig. 2), suggesting that these three cytokines are upregulated by type I EBV latency and might mediate in part the pathogenic potential of EBV. Other cytokines, such as IP-10/CXCL10 and MIP-1β/CCL4, were upregulated in a cell line-dependent manner, which suggests that their expression does not have to be upregulated by EBV during the evolution of BL (Fig. 2).

Somewhat counterintuitively, the production of certain cytokines in EBV-negative BL cells was downregulated by type I EBV latency. The profile of downregulated cytokines was unique to each cell line. In Akata cells, fibroblast growth factor-2 (FGF-2), granulocyte colony-stimulating factor (G-CSF), IL-1α, IL-2, IL-3 and IL-4 were downregulated 2.5- to 3.3-fold (Fig. 2). These cytokines were upregulated during type III EBV latency, which indicates that Akata cells are able to express them. One possible explanation for these results is that EBV expresses a repressor of these cytokines during type I latency in Akata cells, whereas during type III latency, EBV expresses a strong inducer of these cytokines that can counteract the repressor function. In Daudi cells, type I EBV latency resulted in a 3.3-fold decrease in IP-10/CXCL10, whereas in the other two cell lines (Akata and Mutu), IP-10/CXCL10 was upregulated by type I EBV latency (Fig. 2).

Akata and Mutu cells support type III EBV latency. Infection of EBV-negative Akata cells with B95-8 EBV results in type III latency. Mutu cells with type III EBV latency have been isolated *in vitro*, which was a spontaneous shift from type I–III latency. Type III Akata and Mutu cells produced IL-10, IP-10/CXCL10, MDC/CCL22, MIP-1α/CCL3, MIP-1β/CCL4 and RANTES/CCL5 at high levels, a signature that, with the exception of RANTES/CCL5, overlapped that of BL cells (Fig. 1). Type III Mutu cells were unique in that they also produced high levels of IFN-α2 (Fig. 1). Cytokine production in type III BL cells was more active than in type I cells (Fig. 1). The magnitude of IL-10, MDC/CCL22 and MIP-1α/CCL3 induction during type III EBV latency was 48.6-, 5441.8- and 65.1-fold, respectively (average values for two cell lines), in Akata and Mutu cells (Fig. 2). These results suggest that type III latency-associated viral genes are more potent cytokine inducers than those expressed during type I latency. Although the production levels were modest, the many other following cytokines were upregulated in type III BL cells compared with their EBV-negative counterparts: FGF-2, Flt-3L, fractalkine/CX3CL1, IFNγ, IL-1α, IL-1β, IL-1ra, IL-6, IL-8/

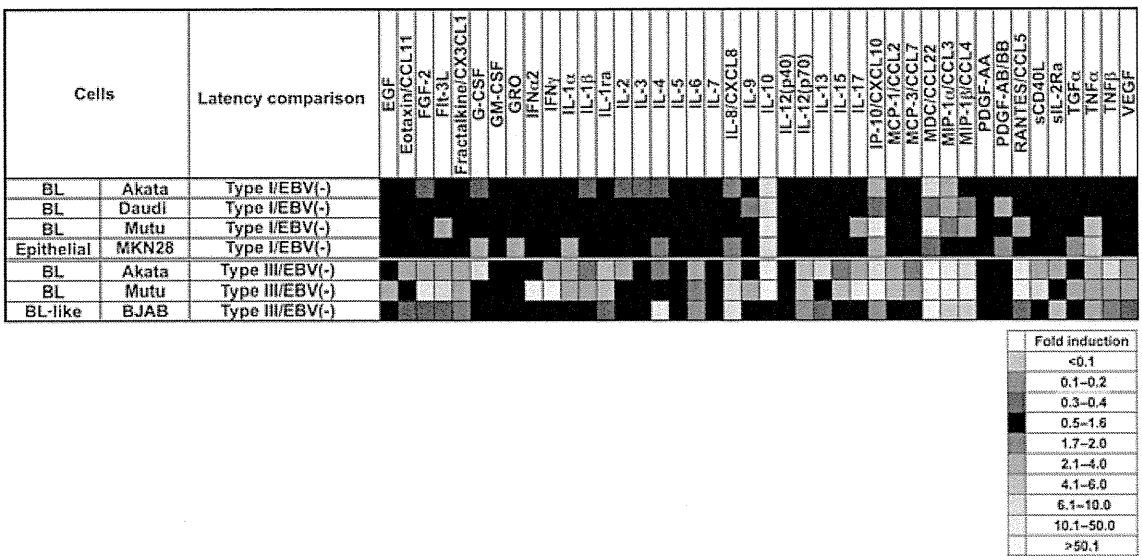

Fig. 2. Induction of cytokine production during type I and type III Epstein–Barr virus (EBV) latency in different B cell lines and an epithelial cell line MKN28. To visualize the magnitude of cytokine induction, the data were color-coded according to fold difference in expression level, as indicated in the legend. Comparisons were between EBV-negative cells and their EBV-positive counterparts. If a cytokine was not detected, the theoretical lower limit of detection, as described by the manufacturer's overnight incubation protocol, was used to estimate the fold-difference value. BL, Burkitt's lymphoma; EGF, epidermal growth factor; FGF, fibroblast growth factor; G-CSF, granulocyte colony-stimulating factor; GM-CSF, granulocyte–macrophage colony-stimulating factor; GRO, growth-related oncogene; IFN, interferon; IL, interleukin; MCP, monocyte chemoattractant protein; MDC, macrophage-derived chemokine; MIP, macrophage inflammatory protein; PDGF, platelet-derived growth factor; RANTES, regulated upon activation, normal T cell expressed and secreted; TGF, transforming growth factor; TNF, tumor necrosis factor; VEGF, vascular endothelial growth factor.

doi: 10.1111/j.1349-7006.2011.01924.x

CXCL8, IL-10, IL-12(p70), IL-15, IL-17, IP-10/CXCL10, MCP-1/CCL2, MCP-3/CCL7, MDC/CCL22, MIP-1α/CCL3, MIP-1β/CCL4, RANTES/CCL5, sCD40L, TNFα, TNFβ and vascular endothelial growth factor (VEGF) (Fig. 2).

Previously, we reported that EBV-encoded small RNA (EBER) play a role in the induction of IL-10 in Akata cells and contribute to their malignant phenotype.[22,32] We investigated whether the expression of EBER was responsible for the induction of type I BL cytokines. The expression of EBER in EBV-negative Akata cells resulted in the upregulation of IL-10 production by approximately 2.5-fold (Fig. 1), consistent with a previous report.[22] However, the levels of MDC/CCL22 and MIP-1α/CCL3 were unaffected by EBER (Fig. 1). These results suggest that an as-yet unidentified viral factor is responsible for the upregulation of MDC/CCL22 and MIP-1α/CCL3. Ectopic expression of EBER also failed to downregulate the levels of FGF-2, G-CSF, IL-1β, IL-2, IL-3 and IL-4 in Akata cells, which suggests that EBER do not function as a repressor of these cytokines during type I EBV latency (Fig. 1).

Cytokine signature of the BL-like cell line BJAB. The BL-like cell line BJAB exhibited a similar cytokine profile to BL cells but with some key differences. Both types of cells produced IL-10, IP-10/CXCL10, MDC/CCL22, MIP-1α/CCL3 and MIP-1β/CCL4 (Fig. 1), which was the BL cytokine signature. This is noteworthy because the histology of BL-like lymphoma is similar to BL, even though BL-like lymphoma does not harbor an Ig/c-myc translocation and is negative for EBV, strongly suggesting the role of BL signature cytokines in the pathogenesis. Unlike the BL cell lines, BJAB cells produced high levels of fractalkaine/CX3CL1, RANTES/CCL5, TNFβ and VEGF (Fig. 1). The level of MDC/CCL22 was substantially lower than the BL cell lines. Thus, the BJAB cytokine signature was distinct from the BL cytokine signature. Epstein–Barr virus infection of BJAB cells, which results in type III latency, was associated with the upregulation of IL-4, IL-8/CXCL8, MDC, sIL-2Ra, TNFα and TNFβ, and downregulation of eotaxin/CCL11, FGF-2, Flt-3L, IL-1ra, IL-6, IL-12(p70), IL-13, IP-10/CXCL10, MIP-1α/CCL3, MIP-1β/CCL4, RANTES/CCL5 and VEGF (Fig. 2). The levels of MIP-1α/CCL3 and MIP-1β/CCL4 production in EBV-infected BJAB cells were markedly reduced to 0.6% and 2.3%, respectively, relative to the uninfected cells (Fig. 2). This strong repression of cytokine production by EBV was unique to BJAB cells. Similar to BJAB cells, EBV also establishes type III latency in Akata and Mutu cells. Type III EBV latency in Akata and Mutu cells did not result in the downregulation of any cytokines (Fig. 2). These results indicated that the cellular genetic background of BJAB, a BL-like lymphoma, differs from that of BL cells. To our knowledge, this is the first report of differences in cytokine production associated with type III EBV latency in BL and BL-like cells.

Previously, it was reported that MDC/CCL22 levels are upregulated upon EBV infection in BJAB cells, and that LMP-1 induces the expression of IL-6, IL-8/CXCL8, IL-10, IP-10/CXCL10, RANTES/CCL5, TNFα and TNFβ.[12,16,17,33–35] In Akata cells, we reproduced the upregulation of these cytokines by LMP-1, although the color code did not show modest upregulation of IL-6, IL-8/CXCL8, TNFα and TNFβ for their low expression levels (2.9-, 6.9-, 8.3-, and 11.0-fold, respectively; Fig. 1). Our data were consistent with these earlier results in terms of induction of IL-8/CXCL8, MDC/CCL22, TNFα and TNFβ by type III EBV latency in BJAB cells, which express LMP-1. However, unlike previous results, type III EBV latency in BJAB cells was not associated with the upregulation of IL-10 and resulted in the downregulation of IL-6, IP-10/CXCL10 and RANTES/CCL5. One explanation for these seemingly controversial results is that there might be viral genes expressed during type III EBV latency in BJAB cells that can counteract the function of LMP-1. It is worth noting that the analysis of viral gene function using transfection assays might not accurately reflect events that are relevant to viral infection.

Cytokine production profile of B-LCL. There were more cytokines produced by B-LCL than BL cells, and the levels of the cytokines produced were higher than in BL cells (Fig. 1). The cytokine profiles varied among B-LCL from different donors, and the cytokine profiles of independent cultures of B-LCL from the same donor also exhibited some variation (Fig. 1). However, almost all the B-LCL produced the following cytokines: IL-8/CXCL8, IL-10, IL-13, IP-10/CXCL10, MDC/CCL22, MIP-1α/CCL3, MIP-1β/CCL4, PDGF-AA, RANTES/CCL5, TNFα, TNFβ and VEGF (Fig. 1). The cytokine signature of the B-LCL was distinct from the BL and BL-like cell lines in that the levels of certain cytokines, namely MIP-1β/CCL4, PDGF-AA, RANTES/CCL5 and TNFβ, were substantially higher (Fig. 1). There was no evidence of virus strain-specific cytokine signatures in B-LCL, in that the cytokine profiles induced by EBV of B95-8 and Akata origin were similar.

Cytokine production footprints for other cell types. To determine the specificity of the BL and B-LCL cytokine signatures, we investigated the cytokine production profiles of PBMC from a healthy donor and several different T cell lines. Cytokine production by naïve PBMC was active and the following cytokines were produced at high levels: granulocyte–macrophage colony-stimulating factor (GM-CSF), growth-related oncogene (GRO), IL-1ra, IL-8/CXCL8, MCP-1/CCL2, MDC/CCL22, sIL-2Ra and TNFα (Fig. 1). Unlike the B-LCL, PBMC were poor producers of IL-10, MIP-1α/CCL3 and TNFβ (Fig. 1). These results suggest that the cytokine signature of PBMC is distinct from that of BL and B-LCL. We also analyzed three acute T cell lymphoblastic leukemia-derived cell lines (CEM, Jurkat and MOLT-4) and the HTLV-1-transformed MT-4 T cell line. The T cell lines produced only a few cytokines, namely VEGF (by MOLT-4 cells), MIP-1α/CCL3, RANTES/CCL5 and sIL-2Ra (by MT-4 cells) (Fig. 1). Importantly, none of the T cell lines produced detectable levels of IL-10, IL-12 (p40), IL-13, MDC/CCL22 and MIP-1β/CCL4, a cytokine phenotype that could theoretically be used to distinguish between tumor cells of T cell and B cell origin (Fig. 1). All four T cell lines exhibited unique cytokine signatures, which suggests that these cell lines are genetically divergent and that the cytokines produced might play distinct roles in the pathogenesis of T cell malignancies. Additionally, we analyzed an epithelial cell line, MKN28, in which EBV establishes type I latency. According to the comparison between EBV-positive and EBV-negative counterparts (Fig. 2), EBV type I latency in MKN28 cells upregulated expressions of G-CSF, GRO, IL-1α, IL-4, IL-8/CXCL8, IL-10 and IP-10/CXCL10, whereas it downregulated expressions of MDC/CCL22, PDGF-AA/BB, sLI-2Ra and TNFα. This profile was unique to MKN28 cells, as highlighted by the reduction of MDC/CCL22, which was increased in all the BL cell lines upon type I EBV latency. Interestingly, however, the induction of IL-10 was consistently seen among all cell lines with type I EBV latency. Overall, the results indicate that the cytokine signatures of BL and B-LCL are unique and can be differentiated from those of other malignancies.

Discussion

In the present study we focused on BL and DLBCL, which occur with relatively high frequency in AIDS patients. Cytokine production profiling revealed that BL cell lines and B-LCL, which represent DLBCL, have unique cytokine signatures (Table 1). Serum IL-6 or IL-10 concentration has been proposed as a diagnostic and prognostic marker for EBV-associated B cell malignancies,[8,15] and profiling more than one cytokine (i.e. IL-6, IL-10 and/or TNFβ) might be more informative than a single

cytokine measurement in terms of a differential diagnosis.[9] The 42 cytokine profiles investigated herein represent a potent diagnostic and prognostic tool. Currently, invasive approaches such as needle biopsy are required to reach a differential diagnosis for B cell malignancies. Serum cytokine profiling is less invasive than current approaches, can be performed rapidly using a microbead-based assay and does not require special expertise to reach a diagnosis, as a pathological examination does. These aspects represent clear advantages to cytokine profiling over current invasive diagnostic procedures. High-throughput cytokine profiling of multiple cytokines represents a potentially useful tool for the differential diagnosis of EBV-associated B cell malignancies with distinct latencies. However, EBV-associated B cell malignancies represent just a subset of all lymphomas. To establish cytokine profiling as a diagnostic tool for all malignant lymphomas, a systematic cytokine analysis of a broad and diverse set of lymphomas is needed.

Cytokines play important roles in the pathogenesis of cancer, including the enhancement of cancer cell proliferation, metastasis, angiogenesis and immune disturbance.[36,37] The cytokines that were upregulated in almost all of the B-LCL and in all of the type I cells are most likely involved in B cell lymphoma pathogenesis. In the case of BL, IP-10/CXCL10 might be involved in part in tissue necrosis and vascular damage.[38] MDC/CCL22 recruits Th2 and regulatory T cells, and might help tumor cells escape Th1-mediated immune surveillance.[38] Although the major function of MIP-1α/CCL3 and MIP-1β/CCL4 is the recruitment of Th1 cells,[38] they might also attract regulatory T cells *in vivo* that help tumor cells counteract host immune defenses.[39] In B-LCL, cytokines such as IL-8/CXCL8, PDGF-AA and VEGF might be involved in local angiogenesis, IL-10 could function as an autocrine/paracrine cell growth factor, and MDC/CCL22, MIP-1α/CCL3, MIP-1β/CCL4, RANTES/CCL5, TNFα and TNFβ might be involved in immune disturbance. The precise roles of these cytokines in the pathogenesis of EBV-associated B cell malignancies remain to be elucidated. Furthermore, the viral gene product(s) responsible for the upregulation of these cytokines should be clarified, as it might lead to novel molecular therapeutic approaches to EBV-associated malignancies.

The BL, BL-like and B-LCL cell lines each differed from the others in their response to type I and III EBV latency. What then is the molecular mechanism underlying these distinct B cell responses to EBV latency? The BL cells are assumed to have originated from the germinal center at late centrocyte stage.[40] The B-LCL are generated from immature-to-mature B cells that express CD21/CR2, a cell surface receptor for EBV. The origin of BL-like lymphoma is not fully understood. The BL-like lymphoma cells and B-LCL do not harbor an Ig/c-myc translocation, as do BL cells. The distinct responses to EBV latency exhibited by each of these cells might be due to differences in their cellular genetic backgrounds that result in differential epigenetic regulation of gene expression, reflected in the induction of certain cytokines by viral genes. Different BL cells exhibited distinct patterns of cytokine regulation during type I or III EBV latency, suggesting that their genetic backgrounds are also different. The unique response of Daudi cells might also be due to the fact that Daudi EBV lacks a part of the viral genome.[41] It remains to be determined whether the peculiarity of BJAB cells to EBV latency is unique to BL-like cells or to BJAB cells.

Using EBV-positive and EBV-negative cells of the same origin, we showed that type I EBV latency results in the upregulation of three cytokines, two of which have been overlooked to date because of the limitations of traditional approaches to cytokine profiling of type I latency. Future studies should be designed to investigate the pathophysiological roles of the BL and B-LCL signature cytokines to better understand the pathogenesis of BL and DLBCL. These cytokines might also represent potential molecular therapeutic targets.

Acknowledgments

The authors thank Kenji Ota and Toru Utsunomiya (Luminex, Japan) for technical assistance. K.M. is a research resident of the Japan Foundation for AIDS Prevention. E.U. is a research resident of Japan–North America Medical Exchange Foundation.

Disclosure Statement

The authors declare no financial or commercial conflict of interest.

References

1 Thompson MP, Kurzrock R. Epstein–Barr virus and cancer. *Clin Cancer Res* 2004; **10**: 803–21.
2 Monroe JG, Silberstein LE. HIV-mediated B-lymphocyte activation and lymphomagenesis. *J Clin Immunol* 1995; **15**: 61–8.
3 Rickinson AB, Kieff E. Epstin–Barr virus. In: Knipe DM, Howley PM, eds. *Fields Virology*, 5th edn. Philadelphia: Lippincott Williams & Wilkins, 2007; 2655–700.
4 Klein E, Kis LL, Klein G. Epstein–Barr virus infection in humans: from harmless to life endangering virus-lymphocyte interactions. *Oncogene* 2007; **26**: 1297–305.
5 Kieff E, Rickinson AB. Epstin–Barr virus and its replication. In: Knipe DM, Howley PM, eds. *Fields Virology*, 5th edn. Philadelphia: Lippincott Williams & Wilkins, 2007; 2603–54.
6 Klein E, Klein G, Nadkarni JS, Nadkarni JJ, Wigzell H, Clifford P. Surface IgM-kappa specificity on a Burkitt lymphoma cell *in vivo* and in derived culture lines. *Cancer Res* 1968; **28**: 1300–10.
7 Emilie D, Touitou R, Raphael M *et al. In vivo* production of interleukin-10 by malignant cells in AIDS lymphomas. *Eur J Immunol* 1992; **22**: 37–2942.
8 Emilie D, Coumbaras J, Raphael M *et al.* Interleukin-6 production in high-grade B lymphomas: correlation with the presence of malignant immunoblasts in acquired immunodeficiency syndrome and in human immunodeficiency virus-seronegative patients. *Blood* 1992; **80**: 498–504.
9 Pastore C, Gaidano G, Ghia P *et al.* Patterns of cytokine expression in AIDS-related non-Hodgkin's lymphoma. *Br J Haematol* 1998; **103**: 143–9.
10 Sharma V, Zhang L. Interleukin-8 expression in AIDS-associated lymphoma B-cell lines. *Biochem Biophys Res Commun* 2001; **282**: 369–75.
11 Nakayama T, Hieshima K, Nagakubo D *et al.* Selective induction of Th2-attracting chemokines CCL17 and CCL22 in human B cells by latent membrane protein 1 of Epstein–Barr virus. *J Virol* 2004; **78**: 1665–74.
12 Uchihara JN, Krensky AM, Matsuda T *et al.* Transactivation of the CCL5/RANTES gene by Epstein–Barr virus latent membrane protein 1. *Int J Cancer* 2005; **114**: 747–55.
13 Maggio EM, Van Den Berg A, Visser L *et al.* Common and differential chemokine expression patterns in rs cells of NLP, EBV positive and negative classical Hodgkin lymphomas. *Int J Cancer* 2002; **99**: 665–72.
14 Setsuda J, Teruya-Feldstein J, Harris NL *et al.* Interleukin-18, interferon-gamma, IP-10, and Mig expression in Epstein–Barr virus-induced infectious mononucleosis and post-transplant lymphoproliferative disease. *Am J Pathol* 1999; **155**: 257–65.
15 Breen EC, van der Meijden M, Cumberland W, Kishimoto T, Detels R, Martinez-Maza O. The development of AIDS-associated Burkitt's/small noncleaved cell lymphoma is preceded by elevated serum levels of interleukin 6. *Clin Immunol* 1999; **92**: 293–9.
16 Nakagomi H, Dolcetti R, Bejarano MT, Pisa P, Kiessling R, Masucci MG. The Epstein–Barr virus latent membrane protein-1 (LMP1) induces interleukin-10 production in Burkitt lymphoma lines. *Int J Cancer* 1994; **57**: 240–4.
17 Vockerodt M, Haier B, Buttgereit P, Tesch H, Kube D. The Epstein–Barr virus latent membrane protein 1 induces interleukin-10 in Burkitt's lymphoma cells but not in Hodgkin's cells involving the p38/SAPK2 pathway. *Virology* 2001; **280**: 183–98.
18 Shimizu N, Tanabe-Tochikura A, Kuroiwa Y, Takada K. Isolation of Epstein–Barr virus (EBV)-negative cell clones from the EBV-positive Burkitt's lymphoma (BL) line Akata: malignant phenotypes of BL cells are dependent on EBV. *J Virol* 1994; **68**: 6069–73.

doi: 10.1111/j.1349-7006.2011.01924.x

19 Nanbo A, Inoue K, Adachi-Takasawa K, Takada K. Epstein–Barr virus RNA confers resistance to interferon-alpha-induced apoptosis in Burkitt's lymphoma. *EMBO J* 2002; **21**: 954–65.
20 Komano J, Sugiura M, Takada K. Epstein–Barr virus contributes to the malignant phenotype and to apoptosis resistance in Burkitt's lymphoma cell line Akata. *J Virol* 1998; **72**: 9150–6.
21 Ruf IK, Rhyne PW, Yang H *et al.* Epstein–Barr virus regulates c-MYC, apoptosis, and tumorigenicity in Burkitt lymphoma. *Mol Cell Biol* 1999; **19**: 1651–60.
22 Kitagawa N, Goto M, Kurozumi K *et al.* Epstein–Barr virus-encoded poly(A)(-) RNA supports Burkitt's lymphoma growth through interleukin-10 induction. *EMBO J* 2000; **19**: 6742–50.
23 Takada K, Horinouchi K, Ono Y *et al.* An Epstein–Barr virus-producer line Akata: establishment of the cell line and analysis of viral DNA. *Virus Genes* 1991; **5**: 147–56.
24 Klein G, Lindahl T, Jondal M *et al.* Continuous lymphoid cell lines with characteristics of B cells (bone-marrow-derived), lacking the Epstein–Barr virus genome and derived from three human lymphomas. *Proc Natl Acad Sci U S A* 1974; **71**: 3283–6.
25 Gregory CD, Rowe M, Rickinson AB. Different Epstein–Barr virus-B cell interactions in phenotypically distinct clones of a Burkitt's lymphoma cell line. *J Gen Virol* 1990; **71**: 1481–95.
26 Maruo S, Yang L, Takada K. Roles of Epstein–Barr virus glycoproteins gp350 and gp25 in the infection of human epithelial cells. *J Gen Virol* 2001; **82**: 2373–83.
27 Miller G, Lipman M. Release of infectious Epstein–Barr virus by transformed marmoset leukocytes. *Proc Natl Acad Sci U S A* 1973; **70**: 190–4.
28 Shimizu N, Yoshiyama H, Takada K. Clonal propagation of Epstein–Barr virus (EBV) recombinants in EBV-negative Akata cells. *J Virol* 1996; **70**: 7260–3.
29 Harada S, Koyanagi Y, Yamamoto N. Infection of HTLV-III/LAV in HTLV-I-carrying cells MT-2 and MT-4 and application in a plaque assay. *Science* 1985; **229**: 563–6.
30 Nakatani H, Tahara E, Yoshida T *et al.* Detection of amplified DNA sequences in gastric cancers by a DNA renaturation method in gel. *Jpn J Cancer Res* 1986; **77**: 849–53.
31 Yoshiyama Y, Imai S, Shimizu N, Takada K. Epstein–Barr virus infection of human gastric carcinoma cells: implication of the existence of a new virus receptor different from CD21. *J Virol* 1997; **71**: 5688–91.
32 Komano J, Maruo S, Kurozumi K, Oda T, Takada K. Oncogenic role of Epstein–Barr virus-encoded RNAs in Burkitt's lymphoma cell line Akata. *J Virol* 1999; **73**: 9827–31.
33 Burdin N, Peronne C, Banchereau J, Rousset F. Epstein–Barr virus transformation induces B lymphocytes to produce human interleukin 10. *J Exp Med* 1993; **177**: 295–304.
34 Herbst H, Foss HD, Samol J *et al.* Frequent expression of interleukin-10 by Epstein–Barr virus-harboring tumor cells of Hodgkin's disease. *Blood* 1996; **87**: 2918–29.
35 Eliopoulos AG, Gallagher NJ, Blake SM, Dawson CW, Young LS. Activation of the p38 mitogen-activated protein kinase pathway by Epstein–Barr virus-encoded latent membrane protein 1 coregulates interleukin-6 and interleukin-8 production. *J Biol Chem* 1999; **274**: 16085–96.
36 Yoshie O, Imai T, Nomiyama H. Chemokines in immunity. *Adv Immunol* 2001; **78**: 57–110.
37 Ben-Baruch A. The multifaceted roles of chemokines in malignancy. *Cancer Metastasis Rev* 2006; **25**: 357–71.
38 Teruya-Feldstein J, Jaffe ES, Burd PR *et al.* The role of Mig, the monokine induced by interferon-gamma, and IP-10, the interferon-gamma-inducible protein-10, in tissue necrosis and vascular damage associated with Epstein–Barr virus-positive lymphoproliferative disease. *Blood* 1997; **90**: 4099–105.
39 Bystry RS, Aluvihare V, Welch KA, Kallikourdis M, Betz AG. B cells and professional APCs recruit regulatory T cells via CCL4. *Nat Immunol* 2001; **2**: 1126–32.
40 Bellan C, Lazzi S, Hummel M *et al.* Immunoglobulin gene analysis reveals two distinct cells of origin for EBV-positive and EBV-negative Burkitt lymphomas. *Blood* 2005; **106**: 1031–6.
41 Jones MD, Foster L, Sheedy T, Griffin BE. The EB virus genome in Daudi Burkitt's lymphoma cells has a deletion similar to that observed in a non-transforming strain (P3HR-1) of the virus. *EMBO J* 1984; **3**: 813–21.

Bioorganic & Medicinal Chemistry 19 (2011) 816–825

Contents lists available at ScienceDirect

Bioorganic & Medicinal Chemistry

journal homepage: www.elsevier.com/locate/bmc

Structural and biochemical study on the inhibitory activity of derivatives of 5-nitro-furan-2-carboxylic acid for RNase H function of HIV-1 reverse transcriptase

Hiroshi Yanagita [a], Emiko Urano [b], Kishow Matsumoto [a], Reiko Ichikawa [b], Yoshihisa Takaesu [a], Masakazu Ogata [a], Tsutomu Murakami [b], Hongui Wu [b,c], Joe Chiba [c], Jun Komano [b], Tyuji Hoshino [a,*]

[a] Graduate School of Pharmaceutical Sciences, Chiba University, 1-33 Yayoi-cho, Inage-ku, Chiba 263-8522, Japan
[b] AIDS Research Center, National Institute of Infectious Diseases, 1-23-1 Toyama, Shinjuku, Tokyo 162-8640, Japan
[c] Faculty of Industrial Science and Technology, Tokyo University of Science, Yamazaki 2641, Noda, Chiba 278-8510, Japan

ARTICLE INFO

Article history:
Received 25 September 2010
Revised 2 December 2010
Accepted 3 December 2010
Available online 9 December 2010

Keywords:
Antiviral drugs
HIV-1 reverse transcriptase
RNase H enzymatic activity
Inhibitors
Dual metal chelation
Nitro-furan carboxylic acid

ABSTRACT

Rapid emergence of drug-resistant variants is one of the most serious problems in chemotherapy for HIV-1 infectious diseases. Inhibitors acting on a target not addressed by approved drugs are of great importance to suppress drug-resistant viruses. HIV-1 reverse transcriptase has two enzymatic functions, DNA polymerase and RNase H activities. The RNase H activity is an attractive target for a new class of antiviral drugs. On the basis of the hit chemicals found in our previous screening with 20,000 small molecular-weight compounds, we synthesized derivatives of 5-nitro-furan-2-carboxylic acid. Inhibition of RNase H enzymatic activity was measured in a biochemical assay with real-time monitoring of florescence emission from the digested RNA substrate. Several derivatives showed higher inhibitory activities that those of the hit chemicals. Modulation of the 5-nitro-furan-2-carboxylic moiety resulted in a drastic decrease in inhibitory potency. In contrast, many derivatives with modulation of other parts retained inhibitory activities to varying degrees. These findings suggest the binding mode of active derivatives, in which three oxygen atoms aligned in a straight form at the nitro-furan moiety are coordinated to two divalent metal ions located at RNase H reaction site. Hence, the nitro-furan-carboxylic moiety is one of the critical scaffolds for RNase H inhibition. Of note, the RNase H inhibitory potency of a derivative was improved by 18-fold compared with that of the original hit compound, and no significant cytotoxicity was observed for most of the derivatives showing inhibitory activity. Since there is still much room for modification of the compounds at the part opposite the nitro-furan moiety, further chemical conversion will lead to improvement of compound potency and specificity.

1. Introduction

A cocktail regimen of therapeutic agents known as highly active antiretroviral therapy (HAART) showed a great advance in the treatment of human immunodeficiency virus (HIV) infectious diseases. The efficacy of this therapy is, however, limited by the emergence of drug-resistant variants of HIV-1. Drug-resistant viruses have become a serious issue in current HIV chemotherapy[1] because HIV-infected disease inevitably requires long-term treatment. One of the effective and practical measures to suppress drug resistance is to produce new anti-HIV drugs that act on the target not addressed by approved drugs. Drugs directly blocking the viral enzymatic activity usually show a high therapeutic performance. RNase H activity of reverse transcriptase (RT) is the enzymatic activity of HIV-1 that no approved drugs still act on. Since it is possible to take an inhibitor of RNase H activity with other approved drugs, the RNase H inhibition is expected to be one of the attractive targets for anti-HIV drugs.[2]

RT is a virally encoded enzyme of HIV-1. RT is a heterodimer of p51 and p66 subunits and has enzymatic functions of DNA polymerase and RNase H activity. That is, this enzyme converts single-strand viral genomic RNA into double-strand DNA. The enzyme also catalyzes the hydrolysis of RNA phosphodiester bonds of RNA hybridized to DNA. Two spacely-separated active sites with the same protein are responsible for these two enzymatic functions respectively. Hence, RT-associated RNase H activity is one of the attractive targets for developing a novel class of antiviral drugs. Furthermore, dual inhibitory of RNase H activity and the activity of RT-associated polymerase or HIV-1 integrase has been reported because of the structural similarity of their catalytic sites.[3–5]

RNase H activity requires the presence of divalent metal cations to be functionalized in catalysis of endo-nucleolytic phosphodiester hydrolysis. Recent crystallographic studies have shown the

* Corresponding author. Tel.: +81 43 290 2926; fax: +81 43 290 2925.
E-mail address: hoshino@faculty.chiba-u.jp (T. Hoshino).

0968-0896/$ - see front matter © 2010 Elsevier Ltd. All rights reserved.
doi:10.1016/j.bmc.2010.12.011

bimetal mode of divalent metal.[6–8] The enzymatic active site contains four carboxylate residues, creating an environment capable of stabilizing two metal ions. Many RNase H inhibitors are assumed to be bound to the catalytic center and interact with divalent metal ions. That is, chelators of these metal ions are regarded as potential inhibitors of the function of HIV-1 RNase H.

Several different scaffolds have been reported as inhibitors of RNase H activity.[9–13] Diketo acids have been well-known chemical structure showing potent inhibitory for two divalent metal-related enzymatic activity initiating endonucleolytic phosphodiester hydrolysis.[14] Therefore, diketo acid structure has served as a starting point for the design and optimization of inhibitors of HIV-1 integrase or influenza endonuclease. Pyrimidinol is one of typical derivatives bearing a scaffold called *N*-hydroxyimide,[15] and it has been reported to be a potent inhibitor of HIV-1 RNase H function, acting through metal chelation at the active site. *N*-hydroxyimides were firstly described as inhibitors of influenza endonuclease, but they also show high potency in biochemical assays of HIV-1 RNase H. An important feature in the structure of pyrimidinol is a six-member ring having a polar atom alignment compatible with diketo acids. The natural product β-thujaplicinol is another scaffold and has been reported to be a highly potent inhibitor of HIV-1 RNase H activity.[16] Using this chemical, the multiple inhibition of HIV-1 enzymes such as HIV-1 integrase and HIV-1 RT-associated polymerase has been investigated. The prominent feature in the structure of β-thujaplicinol is a seven-member ring bonding with two hydroxy groups and one carboxy group.

From an in vitro screening using 20,000 small molecular-weight compounds, we found chemicals that blocked HIV-1 RT-associated RNase H activity.[17] Several analogues bearing the 5-nitro-furan-2-carboxylic acid ester moiety were shown to work as retroviral RNase H inhibitors. Two of the derivatives were capable of suppressing HIV-1 replication in tissue culture. The distinguishable feature in the structure of our 5-nitro-furan-2-carboxylic acid ester is a five-member ring.

To date, no RNase H inhibitors have been approved for clinical use. One of the problems in developing an RNase H active site inhibitor is the absence of a deep pocket into which the inhibitors can be bound.[7,18] This makes it difficult to improve stable and specific binding of compounds to the RNase H catalytic site. Metal ions at the active site, however, are a suitable aiming point for inhibitor binding. A diketo acid inhibitor was shown to be bound in a metal-dependent manner to the RNase H domain of RT.[14,19] Pyrimidinol analogues were designed to chelate the divalent metals of the RNase H domain.[6] β-Thujaplicinol also chelates the two metal ions at the active site.[7] Judging from the structural similarity to pyrimidinol or β-thujaplicinol, derivatives bearing the 5-nitro-furan-2-carboxylic acid ester moiety are assumed to chelate two divalent metal ions as well.

In this study, we examined chemical compounds for anti-HIV drugs blocking RT-associated RNase H enzymatic activity. A variety of compounds were synthesized on the basis of hit chemicals found in in vitro screening in our previous study. Measurement of inhibitory activity with a fluorescence-based assay and theoretical calculation using quantum mechanical (QM) and molecular mechanics (MM) methods suggested the binding mode of the synthesized compounds. The findings of the present study provide a strategy for designing a chemical structure to enhance the inhibitory activity.

2. Methods

2.1. Organic synthesis

Derivatives from a hit compound bearing 5-nitro-furan-2-carboxylic acid were synthesized to obtain chemical analogs showing high inhibitory activity for RNase H. Parts A, B and C of the hit compound shown in Figure 1a were converted into other chemical substitutes. Then compounds **1–53** were synthesized according to the routes shown in the scheme of Figure 1b.

First, chemical modulation was performed for part A. Part A is composed of large hydrophobic substitutes. Compounds **1–28** were prepared by nucleophilic substitution reaction of 5-nitro-2-furoic acid with an α-chloro carbonylate in the presence of DMAP in DMF at 80 °C (eq. 1 of Fig. 1b). Second, chemical modulation was performed for part B, which shows a large hydrophilicity with a nitro-furan moiety. Compounds **29–45** were prepared by experimental conditions similar to those used in the reaction for converting part A. A substitution reaction was carried out using carboxylic acids that contain a nitro group on the aromatic ring (eq. 2 of Fig. 1b). Third, the chemical structure of part C was modulated. Part C is a region connecting parts A and B. 5-Nitro-2-furoic acid was treated with thionyl chloride to generate an acid chloride as an intermediate, followed by reaction of the generated acid chloride with an α-amino acid ester to produce compounds **46–51** (eq. 3 of Fig. 1b). Additionally, two compounds **52** and **53** were prepared to modulate parts A and C with keeping the ester bond. 5-Nitro-2-furoic acid was converted into an acid chloride as an intermediate with thionyl chloride, followed by the substitution reaction of nucleophilic reagents (eq. 4 of Fig. 1b).

2.2. Evaluation of inhibitory activity

Plasmids expressing p66 or p51 of RT with a hexahistidine tag were prepared by cloning a DNA fragment encoding the HIV-1 RT into the pQE-9 vector.[17] The *Escherichia coli* strain BL21(DE3)pLysS was transformed with the plasmids, and protein expression was induced by treatment with 1 mM isopropyl β-D-thiogalactoside for 3 h. For generating heterodimers, bacteria lysates expressing p66 and p51 were mixed prior to purification. A gradient elution was performed using HiTrap HP columns according to the manufacturer's protocol. The yield of the purified protein was estimated using bovine serum albumin as a standard, and the purification was evaluated with Coomassie blue-stained SDS–polyacrylamide gels. The concentration of HIV-1 RT was approximately 1×10^4 units/g, which was determined by a comparison of polymerase activity with an RT standard.[17]

Alternatively, the expression plasmid vector RT69A, which was kindly provided by Professor E. Arnold at Rutsgers University, was used. This plasmid expresses a heterodimer of p66 and p51, which was reported to produce RT crystals with a resolution below 2 Å in X-ray diffraction analysis due to amino residue mutations of F160S and C280S.[20] The *E. coli* strain Rosetta transformed with the RT69 plasmid was incubated at 37 °C. Protein expression was induced by adding 1 mM isopropyl β-D-thiogalactoside at an OD_{600} value of 0.9 and completed by incubation for 3 h after induction. A cell pellet corresponding to 1.5 L of culture was resuspended in 50 mM Tris–HCl at pH 8.0, 600 mM NaCl, and 1% Triton X-114. The bacterial cell membrane was disrupted by sonication. After removing unnecessary disrupted fragments from the lysate by centrifugation, the expressed protein was obtained from the supernant. Since the RT p51 subunit contains an N-terminal hexahistidine tag, RT was purified by using a HiTrap Ni affinity column with an elution buffer containing 500 mM imidazole. The eluted protein fraction was dialyzed overnight against a buffer containing 50 mM Tris–HCl at pH 8.0 and 600 mM NaCl. The dialyzed RT was incubated with HRV 3C protease for 24 h at 4 °C to cleave the hexahistidine tag attached to the N-terminus of the p51 subunit of the heterodimer RT protein. The protein was again purified by Ni-NTA according to the manufacturer's recommendation to remove the uncleaved protein and HRV 3C protease. The RT69 protein was dia-